mtDNA recombination indicative of hybridization suggests a role of the mitogenome in the adaptation of reef building corals to extreme environments

Eulalia Banguera-Hinestroza[1,2], Yvonne Sawall[3], Abdulmohsin Al-Sofyani[4], Patrick Mardulyn[2], Javier Fuertes-Aguilar[5], Heiber Cardenas-Henao[6], Francy Jimenez-Infante[1], Christian R. Voolstra[1**], Jean-François Flot [2**]*

1. Red Sea Research Center, King Abdullah University of Sciences and Technology (KAUST), Thuwal, Saudi Arabia.
2. Ecology and Evolutionary Biology, Université libre de Bruxelles (ULB), Brussels. Belgium.
3. Bermuda Institute of Ocean Sciences (BIOS), Coral Reef Ecology, Bermuda.
4. Department of Marine Biology, Faculty of Marine Sciences, King Abdulaziz University (KAU), Jeddah, Saudi Arabia.
5. Real Jardín Botánico, RJB-CSIC, Plaza de Murillo 2, 28014 Madrid, Spain.
6. Universidad del Valle, Department of Biology. Group of Ecogenetics and Molecular Biology, Cali, Colombia.

*Corresponding author: ebanguer@ulb.ac.be; eulalia.banguera@gmail.com

** Equal contributions

Abstract

Introgressive hybridization, as evidenced by topological incongruence between nuclear and mitochondrial phylogenies, has been broadly recorded in a range of organisms. However, mtDNA recombination following hybridization is rarely found in animals and was never until now reported in reef-building corals. Here we report unexpected topological incongruence among mitochondrial markers in the phylogenetic analysis of *Stylophora* species distributed along broad geographic ranges, including the full latitudinal (2000 km) and environmental gradient (21°C-33°C) of the Red Sea. The analysis of *Stylophora* lineages in the framework of the mitogenome phylogenies of members of the family Pocilloporidae, coupled with analyses of recombination, shows the first evidence of asymmetric patterns of introgressive hybridization associated to mitochondrial recombination in this genus. Hybridization likely occurred between an ancestral lineage restricted to the Red Sea/Gulf of Aden basins and migrants from the Indo-Pacific/Indian Ocean that reached the Gulf of Aden. The resulting hybrid occurs in sympatry with the parental Red Sea lineage, from which it inherited most of its mtDNA (except the recombinant region that includes the *nd6*, *atp6* and mt*ORF* genes) and expanded its range into the hottest region of the Arabian Gulf. Noticeably, across the Red Sea both lineages exhibit striking differences in terms of phylogenetic and phylogeographic patterns, clades-morphospecies association, and zooxanthellae composition. Our data suggest that the colonization of the Red Sea by the ancestral lineage, which involved overcoming the extreme temperatures of the southern Red Sea, likely resulted in changes in mitochondrial proteins, which led to its successful adaptation to the novel environmental conditions.

Key words: Introgressive hybridization, coral reefs, extreme environments, mtDNA recombination, mito-mito incongruence, mito-nuclear incongruence, *Stylophora*, Pocilloporidae, Red Sea.

45 **1. INTRODUCTION**

46

47 Studies of mitochondrial genomes have been of broad relevance for understanding the ecological and
48 evolutionary processes leading to the diversification of organisms (Ballard and Rand, 2005; Chinnery
49 and Hudson, 2013; Kivisild, 2015; Wolff et al., 2016), due particularly to key characteristics such as:
50 maternal inheritance (in most organisms); high mutation rates in triploblastic metazoans (but not in
51 cnidarians and poriferans; cf. Shearer et al. 2002); and lack of recombination (Barr et al., 2005).
52 However, the latter assumption has been challenged by the increasing evidence of mtDNA
53 recombination in animals (Barr et al., 2005; Ladoukakis and Zouros, 2017; Rokas et al., 2003; Tsaousis
54 et al., 2005; Ujvari et al., 2007) with important ecological and evolutionary implications (Dokianakis
55 and Ladoukakis, 2014; Levsen et al., 2016; Passamonti et al., 2013; Rokas et al., 2003; White et al.,
56 2008).

57

58 In natural populations, most evidence for mtDNA and/or nuclear introgression comes from species
59 living at the edge of their geographic range (i.e. marginal ecosystem that often exhibit genetically
60 atypical populations; Johannesson and André, 2006), perturbed habitats, near extreme environmental
61 conditions or in hybrid zones (Brennan et al., 2014; Hellberg et al., 2016; Johannesson and Carl, 2006;
62 Riginos and Cunningham, 2004; Taylor et al., 2015). There is growing evidence in plants, in fungi, and
63 to a lesser extent in animals, that divergent lineages that meet and interbreed in contact zones,
64 particularly after expanding their range as a consequence of climatic or habitat fluctuations, produce
65 hybrids carrying recombinant mitochondrial genomes (Barr et al., 2005) that are able to adapt to new
66 environmental or habitat conditions leading eventually to hybrid speciation (Brennan et al., 2014;
67 Mastrantonio et al., 2016; Riginos and Cunningham, 2004; Taylor et al., 2015).

68

69 Marginal areas such as the Red Sea, a biogeographic *cul-de-sac* extending from the Indian Ocean, are
70 observed to host a high number of hybrid species (Berumen et al., 2017; DiBattista et al., 2016a;
71 Garzón-Ospina et al., 2012; Johannesson and Carl, 2006; Veron, 1995) and therefore offer an interesting
72 playground to study the main factors influencing patterns of diversification and hybrid speciation in
73 extreme environments. The Red Sea ocean basin exhibits a high variability in oceanographic conditions
74 following a N-S gradient along four well-defined oceanographic provinces (Raitsos et al., 2013), ranging
75 from relatively low temperatures in the northern areas (below 23°C) to record summer temperatures up

to 33°C in the southern region (Acker et al., 2008; Moustafa et al., 2014; Raitsos et al., 2013; Sawall et al., 2015, 2014).

In addition, since its inception this region has undergone a complex climatic and geological history. During the last glacial cycles, the Red Sea experienced multiple sea-level fluctuations (Rohling et al., 2013; Siddall et al., 2003) as well as repetitive periods of connection and isolation from the Indo-Pacific, through the Strait of Bab-el-Mandeb in the South (Righton et al., 1996; Rohling et al., 2013; Siddall et al., 2004). These events, together with discontinuous periods of extinction and re-colonization from refuge zones inside and outside the region (Fine et al., 2013; Pellissier et al., 2014), likely played an important role in shaping the geographic distribution of genetic diversity for coral reefs in this oceanic basin, as well as the diversification of their associated fauna (Berumen et al., 2017; DiBattista et al., 2016a, 2016b, 2013). In fact, it has been postulated that corals entered the region during the Miocene –a period characterized by hyper-saline conditions and strong climate change – and after several episodes of post-Miocene migrations (Taviani, 1998). Lineages already inhabiting this area were affected by the successive geological and climatic processes influencing the region (DiBattista et al., 2016a). Repetitive invasions from the Indian Ocean likely enhanced the potential for the encounter of lineages with different genetic backgrounds, increasing the chance for hybridization and therefore hybrid speciation in the unique conditions of this marine zone.

Introgressive hybridization has been reported to be widespread in reef-building corals, with records mostly in the families Acroporidae, Poritidae and Pocilloporidae (Combosch and Vollmer, 2015; Forsman et al., 2017; Hellberg et al., 2016; Johnston et al., 2017; Richards and Hobbs, 2015; Van Oppen et al., 2001; Willis et al., 2006). Indeed, the topological incongruence observed in coral phylogenies might be explained by reticulate evolution due to multiple climatic and see-level changes across geological eras (Van Oppen et al., 2001; Veron, 1995; Vollmer and Palumbi, 2002; Willis et al., 2006). Moreover, it has been proposed that many species occurring in marginal areas and with restricted distribution, such as those endemic of the Indo-Pacific Ocean, might be hybrids (Richards and Hobbs, 2015; Veron, 1995). Even though mtDNA introgression is expected to be more frequent than nuclear introgression, particularly between species occurring in sympatry (Mastrantonio et al., 2016), it has not being reported to date in reef-building corals.

106 The coral genus *Stylophora* (family Pocilloporidae) is widely distributed in the Indo-Pacific and Indian
107 Ocean and comprises a range of a highly plastic morphospecies (Veron, 1995, 2002), which are
108 diversified within four phylogenetic lineages (Flot et al., 2011; Keshavmurthy et al., 2013; Stefani et al.,
109 2011). *Stylophora* is found throughout the entire environmental range of the Red Sea and is represented
110 by several morphospecies: *Stylophora pistillata* (Esper, 1797), *Stylophora subseriata* (Ehrenberg, 1834),
111 *Stylophora wellsi* (also found in Madagascar), *Stylophora kuelhmanni*, *Stylophora danae* and *Stylophora*
112 *mamillata* (Scheer and Pillai, 1983; Veron, 2002). A recent molecular study aiming to identify species
113 boundaries in the genus (Arrigoni et al., 2016) proposes that all these morphospecies belong to one
114 single cohesive molecular lineage.
115
116 Here, we studied the genetic variation of coral species within the genus *Stylophora* and their associated
117 zooxanthellae across the environmental gradients of the Red Sea, spanning over ~2000Km (12 degrees of
118 latitude), and included sequences from other relevant biogeographic regions (i.e. New Caledonia, Great
119 Barrier Reef, Madagascar, Gulf of Aden and Arabian Gulf). A total of 827 sequences were analyzed to
120 understand their genetic diversity, phylogenetic patterns and phylogeographic framework, in addition 281
121 colonies were typified for *Symbiodinium.* We selected this genus given its widespread geographical
122 distribution in the Indo-Pacific region and the presence of several endemic morphospecies in the Red Sea
123 (Veron et al., 2018), which may represent important sources of genetic variability for the future adaptation
124 of reef-building corals under the current threats of climate changes. Our molecular markers included ITS2
125 for *Symbiodinium* and four nuclear (*hsp70*, ITS1, ITS2 and *PMCA*) and five mitochondrial genes for the
126 coral host (mtCR, *cox1*, 12S, 16S and mt*ORF*). Among these markers, the hypervariable mt*ORF*, a
127 mitochondrial open reading frame of unknown function, which is unique to the family Pocilloporidae (Flot
128 and Tillier, 2007a), has been proposed as an alternative barcode for members of this family, performing
129 as well as NGS sequencing data for distinguishing species (i.e RAD-seq markers; Johnston et al., 2017).
130 But some authors such as Chen et al. (2008) considers the mt*ORF* as the control region, resulting in some
131 confusion in the literature.
132
133 Subsequently, the patterns of diversification of the Red Sea specimens were evaluated using full
134 mitochondrial genome sequences of species belonging to the family Pocilloporidae (*Pocillopora*,
135 *Seriatopora*, *Stylophora* and *Madracis*) (Veron and Pichon 1976). Our aims were (1) to investigate
136 patterns of diversification in *Stylophora* species and their associated zooxanthellae within the Red Sea and

137 verified further whether host morphological variation had any taxonomic value for these species (in other
138 words, is there any association between morphological and genetic variation?). (2) to find out whether
139 mitochondrial variation and phylogeographic patterns fit the trends expected from the environmental
140 gradients in this marginal basin, and (3) to test whether the topological incongruence between mtDNA
141 markers observed in our data and previously reported by Arrigoni et al. (2016) could be explained by
142 introgressive hybridization. Here we discuss our results from an integrative perspective, coupling
143 phylogenetic and phylogeographic patterns, *Symbiodinium* distribution, morphospecies-clades association
144 and the finding of mtDNA recombination. We discuss the implications of these results for coral
145 conservation in highly variable environments.
146
147 **2. MATERIAL AND METHODS**
148
149 **2.1. Coral Sampling**
150
151 We sampled a total of 725 colonies of *Stylophora* at 25 locations along the Red Sea coast in 2011 and
152 2012 from the Gulf of Aqaba in the North (Maqna, 28° 31' 34.20 N, 34° 48' 14.30" E) to Farasan Island
153 in the South (16° 31' 38.5" N, 42° 01' 54.09" E). Our sampling design covered the entire environmental
154 gradient (Temperature: ~21 in the north to ~33°C in the south; Salinity: 41 PSU in the north to 37 PSU
155 in the south) of the Red Sea and the four oceanographic provinces as defined in Raitsos et al. (2013;
156 Figure 1 and Supplementary Table *S1*). Colonies were determined to belong to morphotypes of *S.*
157 *pistillata*, *S. subseriata*, *S. danae*, *S. kuelhmanni* and *S. wellsi* (Figure 1). Identification was carried out
158 with the assistance of Dr. J.E.N Veron (personal communication) and by comparing his photographic
159 records of Red Sea samples with our photographs taken during coral sampling. Small coral nubbins
160 (~1cm) were collected in 3-7 m depth from colonies 5 m apart from each other to minimize sampling of
161 clones and were preserved at room temperature in salt-saturated DMSO buffer (Gaither et al., 2011;
162 Seutin et al., 1991)
163
164 **2.2. DNA extraction, PCR and sequencing**
165
166 Coral nubbins were placed in approximately 400 µL of lysis buffer (DNeasy Plant Minikit; Qiagen,
167 Hilden, Germany®) with sterile glass beads and beaten for 30 s at full speed in a Qiagen Tissue Lyser II

168 (Qiagen, Hilden, Germany®). After cell lysis, DNA was extracted following the protocol recommended
169 by the manufacturer. Five mitochondrial genes and four nuclear genes were amplified. First we barcoded
170 our samples using the mt*ORF*, which is considered the most variable gene for Pocilloporidae (Flot and
171 Tillier, 2007) and a short fragment of the adjacent ATPase subunit 6 gene (*atp6*). After this initial
172 barcoding step, the mitochondrial control region (CR), the cytochrome *c* oxidase subunit I (*cox1*) and
173 the mitochondrial 12S and 16S ribosomal RNA (rRNA) genes were amplified for a subset of samples. A
174 subset was also amplified for several nuclear genes: the heat shock protein (*hsp70*) gene, the internal
175 transcribed spacers (ITS1 and ITS2) and the Plasma Membrane Calcium ATPase (*PMCA*) gene. The
176 16S, 12S and *cox1* were amplified with primers designed in this study. The primers we included and
177 their respective references are listed in the Supplementary Table *S2*.
178
179 After amplification, samples were cleaned using the Exostar 1-step protocol (Ilustra®) and sequenced in
180 both forward and reverse directions; 5-10 specimens of each haplotype were sequenced twice to confirm
181 the accuracy of the sequences. The forward and reverse chromatograms were assembled and edited
182 using Chromas-Pro software version 2.1.5.1 (Technelysium, Pty Ltd). Sequences were first aligned
183 using MUSCLE (Edgar, 2004) as implemented in MEGA version 7.0.26 (Kumar et al., 2016) and when
184 the resulting alignment contained multiple gaps we used MAFFT's FFT-NS-i (Slow; iterative
185 refinement method) to improve the alignment (Katoh and Standley, 2013). All alignments were
186 confirmed and corrected by eye and sequences were trimmed to the same length for further analyses. For
187 12S and 16S, we removed a small region in which a long stretch of homopolymers did not allow high
188 confidence in the alignment. Nuclear genes were phased using the programs PHASE Version 2.1
189 (Stephens and Donnelly, 2003) using the input files obtained in SeqPHASE (Flot, 2010).
190
191 In the few cases when ITS1, ITS2, or *PMCA* chromatograms showed multiple double peaks (as expected
192 when sequencing a mixture of DNA sequences of unequal length; Flot et al., 2006) the indels from these
193 chromatograms were not considered for downstream analyses and only clean regions with double peaks
194 were included in the phasing process. In addition to our samples from the Red Sea, we amplified and
195 sequenced the 12S and 16S markers of selected specimens from Flot et al. (2011) from several
196 geographic regions (New Caledonia, Japan, Philippines and Madagascar). Moreover, previously
197 published mt*ORF* and CR sequences (Flot et al., 2011; Stefani et al., 2011) as well as *hsp70* sequences
198 (Klueter and Andreakis, 2013) from other geographic regions (i.e. Gulf of Aden and Indo-Pacific) as

199 well as from the Red Sea (i.e. mt*ORF* sequences belonging to *S. mamillata*: Arrigoni et al., 2016) were
200 downloaded from the NCBI database and included in our analyses (accession numbers for these samples
201 can be found in the respective references). Finally, we also included *cox1* sequences from Keshavmurthy
202 et al. (2013) that were downloaded from the Dryad Digital Repository: (doi:10.5061/dryad.n2fb2).
203
204 **2.3. Identification of zooxanthellae (*Symbiodinium*)**
205
206 *Symbiodinium* types were identified by the amplification of the *ITS2* rDNA in a set of *Stylophora*
207 samples from the Red Sea collected throughout the same gradient as described above (N=281). We used
208 the DGGE-ITS2 protocol described in LaJeunesse (2002) with the primers and protocols recommended
209 in LaJeunesse et al. (2003). DGGE gels, electrophoresis and PCR conditions are fully described in Arif
210 et al. (2014). Sequences were processed using Chromas-Pro software version 1.7.5 (Technelysium, Pty
211 Ltd) and phylogenetic assignments were built by comparisons with previously published *ITS2* sequences
212 in the GeoSymbio data base (Franklin et al. 2012) and the Todd LaJeunesse's database
213 (https://131.204.120.103/srsantos/symbiodinium/sd2_ged/database/views.php).
214
215 **2.4. Sequence variation, phylogenetic and phylogeographic analyses**
216
217 Number of haplotypes (h), polymorphic sites per gene, and shared haplotypes within and among Red
218 Sea regions (Maqna, Al-Wajh, Yanbu, Kaust, Jeddah, Doga, Farasan, Gulf of Aden; Figure 1) as well as
219 for other geographic locations (see above), were calculated using Arlequin version 3.5 (Excoffier and
220 Lischer, 2010) and DNAsp version 5.1 (Librado and Rozas, 2009). Phylogenetic analyses were
221 performed using *Stylophora* specimens from seven geographic regions (Caledonia, Japan, Philippines,
222 Madagascar, Gulf of Aden, Arabian Gulf and Red Sea). When several sequences shared the same
223 haplotype, a single representative was included in the data set for phylogenetic analyses.
224 To account for the phylogenetic signal in indels (insertion-deletion polymorphism) gaps were treated as
225 missing data and coded as additional presence/absence (0-1) characters with the program Fastgap v1.2.
226 (Borchsenius 2009) resulting in a data set with two data partitions: nucleotides and standard characters
227 (0-1). This approach was used to infer Bayesian trees with a mixed model, which allows the
228 combination of different data partitions with parameters unlinked across partitions (Huelsenbeck and
229 Ronquist, 2001). The best evolutionary models for each gene and data partition were selected by

230 calculating their BIC (Bayesian Information Criterion) scores as recommended in MEGA v.7 (Kumar et
231 al. 2016). The non-uniformity of evolutionary rates among sites was modelled using a discrete Gamma
232 distribution (+G) with 5 rate categories and by assuming a portion of the sites to be invariant (+I). The
233 gamma shape parameter, proportion of invariant sites, transition/transversion ratio, nucleotide
234 frequencies and rates of substitutions were also estimated from the data.
235
236 Bayesian trees were built in MrBayes (Huelsenbeck and Ronquist, 2001) at the CIPRES Science
237 Gateway v 3.1 (Miller et al., 2010). For each data set we performed 4 independent runs (nruns=4) with 1
238 cold and 3 heated chains (nchains=4). The total number of generations (ngen) was set at 10,000,000;
239 sampling was performed every 1000 generations (Diagnfreq=1000); and the burn-in fraction was set to
240 25% (burninfrac=0.25). Convergence was assessed using the program Tracer v 1.7 (Rambaut and
241 Drummond, 2009). Maximum Likelihood (ML) and Neighbor Joining (NJ trees) were built in MEGA v7
242 (Kumar et al., 2016), with 1000 bootstrap replicates, We used the nearest neighbor interchange
243 algorithm (NNI) with an initial tree automatically generated (option: NJ/BioNJ) and the branch-swap
244 filter set to strong, including all sites in the alignment. NJ trees were constructed using the Maximum
245 Composite Likelihood method, with the pairwise deletion option activated. Trees were constructed for
246 all markers, except 16S and *cox1* that showed little or no variability in *Stylophora* spp. (see results).
247 mt*ORF* and CR phylogenies (using our complete data set) were built only using the alignable regions
248 among all samples and the outgroups (*Pocillopora* and *Seriatopora*), and alternatively, excluding the
249 outgroups to allow the analyses of longer fragments (in these cases, the root of the trees was placed in
250 agreement with that inferred by the phylogeny using shorter fragments and by the loci in which the full
251 outgroup sequences were included).
252
253 Relationships among haplotypes were explored for the three most variable markers (mt*ORF*, CR and
254 *hsp70*) using the program HaplowebMaker (https://eeg-ebe.github.io/HaplowebMaker/; Spöri and Flot,
255 in prep.) applying the median-joining algorithm. Haplotypes belonging to specimens from the Pacific
256 regions and Madagascar were included, when possible, to identify patterns of colonization. The
257 frequency of each haplotype along the environmental gradient of the Red Sea (i.e. each
258 locality/population) was calculated using Arlequin v. 3.5 (Excoffier and Lischer, 2010).

259 **2.5. Mitogenomes assembly and annotation**

260

261 The complete mitogenomes of the two Red Sea lineages identify in our individual phylogenies analyses
262 (see results) –called *RS_LinA* and *RS_LinB* hereafter– were obtained using two different approaches.
263 First, paired-end Illumina reads from the draft genome of *Stylophora pistillata* (Voolstra et al. 2017)
264 –identified as *RS_LinA*– were downloaded from the NCBI Short Read Archive
265 (https://www.ncbi.nlm.nih.gov/sra/SRX999949) using fastq-dump (fastq-dump --origfmt --split-3
266 SRR1980974). Second, 1.7 Gb paired-end reads for the *RS_LinB* were obtained from Red Sea samples
267 preserved in CHAOS buffer (Flot 2007) and extracted using the DNA NucleoSpin kit (Macherey-
268 Nagel) following the protocol recommended by the company. Sequencing was performed in an Illumina
269 NovaSeq 6000 at the BRIGHTcore facilities (Brussels Interuniversity Genomics High Throughput core)

270

271 The mitogenome of both lineages were assembled de novo from the raw Illumina reads using
272 NOVOPlasty v2.7.1 (Dierckxsens et al., 2016) with the *cox1* gene as a seed. For the assembly of the
273 *RS_LinB* mitogenome, both *cox1* and the complete mitogenome of the *RS_LinA* were used as seeds.
274 Runs were performed without and with reference, using the mitogenome of *Stylophora pistillata*
275 (NC_011162.1) for comparative purposes. The accuracy of the assembly was confirmed by mapping the
276 reads back to the assembled genomes using Bowtie2. In addition, the identity of each lineage was
277 corroborated by aligning the resulting genomes with sequences from six of the markers used for our
278 interspecific phylogenies (mt*ORF*, CR, *atp6*, 12S, 16S and *cox1*). Genes were annotated using MITOS
279 (Al Arab et al., 2017; Bernt et al., 2013). Alignment for each annotated gene was performed with
280 MUSCLE (Edgar, 2004) and genes identities were confirmed using BLAST searches. When there was
281 incongruence, particularly at the 5' and 3' ends of the genes, annotations were manually corrected using
282 as reference standard (RefSeq) the mitogenome of *Stylophora pistillata* from the NCBI data base
283 (NC_011162.1). Finally, genes were concatenated using Fastgap v1.2. (Borchsenius 2009) and aligned
284 with mitogenomes from other members of the family Pocilloporidae using MAFFT (Katoh and Standley,
285 2013). The mitogenomes included were: *Seriatopora hystrix* (EF633600.2), *Seriatopora caliendrum*
286 (EF633601.2), *Pocillopora damicornis* (EF526302.1; EU400213.1), *Pocillopora eydouxi* (EF526303.1),
287 *Stylophora pistillata* (of Indo-Pacific origin; NC_011162.1) and *Madracis mirabilis* (EU400212.1).

288 **2.6. Analyses of recombination and mitogenome phylogenies**

289

290 Recombination was tested using the alignments of the full mitogenomes from members of the family
291 Pocilloporidae, including the two divergent *Stylophora* lineages from the present study –see results –;
292 the genus *Polyciathus* was also included as an external sequence. Seven heuristic recombination
293 detection methods implemented in the RDP4 package (Martin et al., 2015) were used: RDP (Martin et
294 al., 2010), BOOTSCAN (Martin et al., 2005), GENECONV (Padidam et al., 1999), MAXCHI
295 (Maximum Chi Square method; Smith 1992); CHIMAERA (Posada and Crandall, 2001), SISCAN
296 (Sister Scanning method; Gibbs et al. 2000), and 3SEQ (Boni et al., 2006).

297

298 The default settings were used for most methods, except for window sizes, step sizes and tree building
299 methods. Window size was selected to include at least 10 variable nucleotide positions within every
300 window examined. In RPD, SISCAN, and BOOTSCAN methods windows size were set at 100; in
301 CHIMAERA and MAXCHI at 200. Alternatively, the MAXCHI and CHIMAERA methods were set to
302 run with variable windows sizes, to allow the program to adjust the window size depending on degrees
303 of parental sequence divergence as recommended by the author. Only recombination events detected
304 with $P<0.05$, after Bonferroni correction were recorded.

305

306 The boundaries of the breakpoints were double checked by comparing the agreement of the boundaries
307 between methods. The major parent and the minor parent hypothesized by the program, were contrasted
308 against evidence from our phylogenetic and phylogeographic analyses. Furthermore, given that the
309 parental ascription of the recombinant sequence may be difficult among closely related sequences, we
310 refined the hypothesis by comparing the hypothesized distribution range of the major *Stylophora* clades
311 (Keshavmurthy et al., 2013) and the supporting data from previous studies in hybrids species in the
312 region and outside the Red Sea (DiBattista et al., 2015). It is important to note that the identified major
313 and minor parents are not the "real" parental sequences, but sequences that are closely related to likely
314 ancestral sequences, also that the recombinant region is related to the "minor" parent and the "non-
315 recombinant" region related to the "major" parent (Martin et al., 2015).

316

317 Phylogenetic relationships among mitogenomes were inferred using maximum likelihood trees in
318 PhylML (Guindon et al., 2010) available at the http://www.phylogeny.fr/index.cgi (Dereeper et al.,

319 2010, 2008). Branch support was evaluated using an Approximate Likelihood Ratio test (aLRT)
320 (Anisimova and Gascuel, 2006). Trees were built for: (a) the full alignments, including and excluding
321 the recombinant region and (b) genes within the recombinant region. The best model was selected as
322 indicated in MEGA v7 (Kumar et al., 2016) as the GTR+G+I (General Time Reversible mode, non-
323 uniformity of evolutionary rates among sites modeled using a discrete Gamma distribution with 5 rate
324 categories and a fraction invariable sites). Because ambiguously aligned regions or highly divergent
325 sequences can mislead recombination signals, we ran the analyses including and excluding the *mtORF*
326 and the *atp8* gene, and also excluding ambiguously aligned regions within the mt*ORF*. Finally, to
327 discard the influence of highly divergent sequences, we repeated the recombination analyses excluding
328 the mitogenomes of *Madracis* and *Polyciatus* species. After analyses, polymorphic sites in hypervariable
329 genes within the recombinant region for each *Stylophora* were calculated using DNAsp version 5.1
330 (Librado and Rozas, 2009).
331
332 **3. RESULTS**
333
334 **3.1. Gene variation and polymorphic sites**
335
336 Our largest data set consisted of 827 sequences of the mt*ORF* locus, which includes a short region of the
337 adjacent *atp6* gene, from a large portion of the geographic distribution of *Stylophora* (Figure 1); it
338 included 716 samples from our collection of the Red Sea, 3 samples from the Arabian Gulf, plus 108
339 sequences of *S. pistillata* morphospecies from Stefani et al. (2011) and Flot et al. (2011): from the Gulf
340 of Aden (N=20), Pacific regions (N=60) and Madagascar (N=28). In addition, we produced a second
341 dataset for four other mitochondrial fragments, from CR (N=401), *cox1* (N=147), 12S (N=72) and 16S
342 (N=61) and four nuclear fragments, from *hsp70* (N=738), ITS1 (N=75), ITS2 (N=56) and *PMCA*
343 (N=86) genes. This data set includes sequences from other studies (see material and methods section 2).
344
345 While the *atp6*-mt*ORF* locus (N=827; 884-943 bp) displayed a high level of polymorphism in
346 *Stylophora* samples, the two *cox1* fragments (303-545 bp) were found monomorphic when comparing
347 sequences across all Red Sea specimens. Pairwise comparisons among all individuals uncovered
348 multiple synonymous and non-synonymous substitutions at the 5' end and 3' end of the mt*ORF* gene,
349 but noticeably, the core region was composed mainly by duplicated tandem repeats, which were of

350 variable lengths and dissimilar among *Stylophora* specimens from the Red Sea (in terms of nucleotide
351 composition and length of the repeat; data not shown). The CR (N=401; 757 bp) was the most variable
352 of the non-coding markers, with polymorphism mainly caused by variation in the number of tandem
353 repeats, some of them being specific to *Stylophora* specimens inhabiting different geographic areas.
354 Polymorphic sites, indels and parsimony informative sites for mitochondrial and nuclear genes are
355 recorded in Supplementary Table *S3*.
356
357 **3.2. Phylogenetic analyses**
358
359 ML and Bayesian phylogenies inferred from the *atp6*-mt*ORF* locus including *Pocillopora* as an
360 outgroup (no shown) or excluding the outgroup (Figure 2a) showed a large phylogenetic subdivision
361 between two groups, each associated with both high Bayesian Posterior Probabilities (BPP > 1.0) and
362 high bootstrap values (> 99%). A first clade, (N=461; h=27) included some of the sequences from the
363 Red Sea and the Gulf of Aden and those from the Arabian Gulf (N=373; h=12), plus sequences from
364 Madagascar (N=28, h=6) and the Pacific (N=60; h=9); the second clade included the other specimens
365 from the Red Sea and Gulf of Aden (N=366; h=14) –we refer to this clade as the Red Sea Lineage B
366 (*RS_LinB*)– (Figure 2a). These two lineages were also evident in the mitogenome phylogenies of the
367 family using the full *atp6* (678 bp) and *nd6* genes (564 bp) (Figure 3a) and in the phylogenies derived
368 from our recombination analyses (Figure 3b) –See recombination results below–. In fact, the *atp6* gene
369 revealed 50 and 45 polymorphic sites between *RS_LinB vs RS_LinA* and *RS_LinB* vs Indo-Pacific/Indian
370 Ocean lineage respectively, and only 8 polymorphic sites between *RS_LinA* and the Indo-Pacific/Indian
371 Ocean lineage.
372
373 In contrast, in the phylogenetic trees inferred from all other markers, whether mitochondrial (CR, 12S)
374 or nuclear (ITS1; ITS2*, hsp70; PMCA*) (Figures 2b and Supplementary Figure *S1*), *RS_LinA* and
375 *RS_LinB* sequences form a clade that exclude all sequences from Madagascar and from the Indo-Pacific
376 region. There is therefore a major incongruence between the phylogenetic signal of *atp6*, *nd6* and the
377 mt*ORF* vs the CR and 12S (Figure 2 and Figure 3a) and between mtDNA genes vs the nuclear genes.
378 The ITS2 showed a pattern similar to that of the CR, in which *RS_LinA* and *RS_LinB* are almost
379 completely separated; there is only one individual from *RS_LinB* placed inside the clade formed by

380 *RS_LinA* sequences, and vice versa, on the ITS2 tree (Supplementary Figure *S1*). The *cox1* and the 16S
381 trees provided only little phylogenetic information (not shown).
382
383 **3.3. Comparative analyses between *RS_LinA* and *RS_LinB***
384
385 **3.3.1. Intraspecific phylogenies and morphospecies-clade association**
386
387 Bayesian and ML trees obtained based on the full-length sequences of the *atp6*-mt*ORF* locus, thus
388 analyzing members of each lineage (*RS_LinA,* 884 bp, h=33; *RS_LinB*, 943 bp, h=20) separately, are
389 shown in Figure 4. In general, we found no clear association between Red Sea morphospecies and
390 phylogenetic groups in the *RS_LinA* lineage. For example, some mitochondrial haplotypes were shared
391 among different morphotypes or/and individuals exhibiting the same morphotypes were placed into
392 different subclades (Figure 4a); the only exceptions were haplotypes belonging to morphotypes of *S.*
393 *kuelhmanni*, that were all associated with subclade *LA1*, and those from *S. mamillata* –from Arrigoni et
394 al. (2016)– that were exclusively found in subclade *LA3* (data not shown). Instead, in the *RS_LinB*
395 lineage, morphotypes attributed to *S. subseriata* (called *Stylophora* cf. *subseriata* thereafter) were
396 grouped in subclade *LB1* and displayed haplotypes found exclusively in the northern Red Sea –see
397 phylogeographic analyses below– and were differentiated from morphotypes belonging to *S. pistillata*
398 (mainly short and medium branched morphotypes, called as *Stylophora* cf. *pistillata* from now on),
399 whose haplotypes were distributed mainly in the central-southern Red Sea and were placed in subclade
400 *LB2* (Figure 4b).
401
402 **3.3.2. *Symbiodinium* distribution**
403
404 As for zooxanthellae, *Symbiodinium* type A1 (*Symbiodinium microadriaticum*) was the most abundant
405 in members of *Stylophora* within the Red Sea (167 out of 281 colonies), followed by *Symbiodinium* type
406 C160 (N=49). The distribution of these types was somehow different between members of each
407 *Stylophora* mtDNA lineage (Figure 4). In colonies placed within the *RS_LinB* and inhabiting the
408 northern Red Sea (i.e. subclade *LB1*; *Stylophora* cf. *subseriata*; N=76) the most abundant type was C160
409 (N=41) followed by type A1 (N=22) and few colonies presented both types (A1-C160; N=9). In
410 contrast, colonies distributed in the central-southern areas (i.e. subclade *LB2*; i.e. *Stylophora* cf.

411 *pistillata*) were mainly associated with type A1 (40 out of 54 colonies) and the presence of C160 type,
412 or of this type in combination with A1 (A1-C160) were not detected. In southern regions, few colonies
413 exhibited the C1* type, which was not present in northern colonies and was always found in association
414 of type A1 (i.e. A1-C1*; N=10). Other C types or associations A1-C types were found in very low
415 abundance (i.e. in one colony). A high percentage of the colonies of the *Stylophora RS_LinA* (105
416 colonies out of 151) showed association with *Symbiodinium microadriaticum* in both northern and
417 southern regions. The few colonies carrying C160 or A1-C160 types were mainly found in Yanbu (7 out
418 of 11 colonies). The presence of C1* and A1-C1* types were detected mostly in colonies inhabiting the
419 southernmost area of the Red Sea (i.e. Farasan; 7 out of 8 colonies). Few C types (i.e. C161, C162,
420 C116) and combination of A1 with other types (i.e. A1-D, A1-C41, A1-B, A1-C1, A1-C19; A1-sp)
421 displayed low frequencies and some of them were exclusive of colonies belonging to this group (Figure
422 4).
423
424 **3.4. Comparative phylogeography of *RS_LinA* and *RS_LinB* and patterns of genetic variation**
425 **along the Red Sea gradient**
426
427 Median-joining networks were constructed for the markers for which we had the largest number of
428 sequences: *atp6*-mt*ORF* (N=827), CR (N=401) and *hsp70* (N=738). Each network indicates a clear
429 phylogeographic signal (i.e., there was a visible association between genetic variation and geographic
430 location). The north-south genetic differentiation was more pronounced for *RS_LinB* than for *RS_LinA*,
431 a pattern supported by all three loci (Figure 5). Haplotype frequencies along the gradient were somehow
432 different among lineages. In *RS_LinB* the highest frequencies of the most common haplotypes were
433 found either in northern or southern areas, while haplotype frequencies in *RS_LinA* showed a clinal
434 variation (Supplementary Figure *S2*). For the *hsp70*, haplotypes showed different frequencies along the
435 gradient when evaluated per mtDNA lineage (Supplementary Figure *S2c*) and the pattern was similar to
436 that shown by the *atp6*-mt*ORF* locus.
437
438 **3.5. mtDNA recombination analyses**
439
440 The analyses of the mitogenomes for all members of the family Pocilloporidae including *RS_LinA* and
441 *RS_LinB* and the genus *Polycyathus*, resulted in the detection of several recombination events in

442 pocilloporid corals. Recombination signals were detected in *Stylophora, Seriatopora and Madracis.* The
443 signals for *Stylophora* and *Seriatopora* were confirmed when excluding the two divergent genomes of
444 *Madraci*s and *Polycyathus*. In *Stylophora* the strongest signal supported by all seven methods was found
445 in *RS_LinA*, with the major parent hypothesized as the *RS_LinB* and the minor parent *Stylophora*
446 *pistillata* (Taiwan). *P*-values were as follow: RDP = 1.175×10^{-10}; GENECONV = 8.96×10^{-11};
447 BOOTSCAN = 1.237×10^{-11}; MAXCHI = 7×10^{-16}; CHIMAERA = 4.019×10^{-03}; SISCAN = $1.090 \times$
448 10^{18} and 3SEQ = 2.969×10^{-29}. The boundaries of the breakpoints were placed at the end of the *nd2*
449 genes by all methods, extending across the *nd6*, *atp6*, mt*ORF* and ending at the beginning of the *nd4*
450 gene (Supplementary Figure *S3*). A second event, in which the recombinant region was transferred from
451 *Pocillopora* to the *RS_LinB* was hypothesized, in this case the recombinant region was restricted to the
452 *atp6* gene. A third event was detected, by only 3 methods, in *Seriatopora hystrix and Seriatopora*
453 *caliendrum*.
454
455 Family phylogenies focused in *Stylophora* and including the region inherited from the minor parent (*S.*
456 *pistillata*, Taiwan; 2415 bp) and the major parent (*RS_LinB*; 9555 bp) (Figure 3b) corroborated the
457 phylogenetic patterns outlined for *RS_LinA* and *RS_LinB* in our interspecific phylogenies (Figure 2).
458
459 **4. DISCUSSION**
460
461 The results from our study show support for the hypothesis that mtDNA introgressive hybridization is
462 the most likely cause of topological mito-mito incongruence in *Stylophora*. Our recombination analyses,
463 using the full mitogenomes of pocilloporid corals (*Madracis, Pocillopora, Seriatopora* and *Stylophora*,
464 including the two Red Sea lineages), provides evidence of mtDNA introgression in this group –
465 particularly in *Stylophora*– strongly suggesting the existence of a hybrid lineage (*RS_LinA*) in the Red
466 Sea, Gulf of Aden and Arabian Gulf. The mitogenome of this lineage contains introgressed genes from
467 two divergent mitochondrial lineages: on mtDNA genes found in the recombinant region (i.e. covering
468 the complete *nd6*, *atp6* and mt*ORF* genes), which have been inherited from a parental species included
469 in a lineage distributed in the Indo-Pacific/Indian Ocean region, while all other mtDNA genes can be
470 traced back to the ancestor of the *RS_LinB*. In the Red Sea, the *RS_LinA* is found in sympatric
471 association with the descendants of its local parental species (*RS_LinB)*, and they harbour different
472 phylogeographic patterns and different *Symbiodinium* composition. In addition, we found that

473 morphospecies placed within the *RS_LinB* agreed with phylogenetic subclades, which accounts for the
474 presence of two divergent allopatric populations divided in northern and southern areas, consistent with
475 environmental and oceanographic discontinuities, a trend that was completely absent in the hybrid
476 *RS_LinA*.
477
478 The colonization of the extreme environments of Red Sea by the ancestral *RS_LinB* implied the
479 development of adaptations to demanding temperature and salinity conditions. This likely involved
480 selective pressures observed to multiple amino acid changes in mitochondrial proteins, evidenced by the
481 highest substitution rate in the *atp6* and in the mt*ORF* genes of the *RS_LinB*, when compared with other
482 *Stylophora* lineages, which suggest a role of such mtDNA genes in the adaptation to extreme
483 environments. These results have important implications for the conservation of Red Sea species and
484 corals.
485
486 **4.1. Divergent mitochondrial lineages of *Stylophora* are present in the Red Sea**
487
488 Our *atp6*-mt*ORF* phylogenetic analyses highlight the presence of two divergent sympatric *Stylophora*
489 lineages in the Red Sea/Gulf of Aden/Arabian Gulf areas: the *RS_LinA* sharing a common ancestry with
490 an Indo-Pacific/Indian Ocean/Madagascar lineage –placed in Clade 1– and the *RS_LinB* lineage, which
491 form a unique clade on its own –Clade 2– (Figure 2). These lineages were also supported by the family
492 phylogenies of the *atp6* and *nd6* genes (Figure 3a). Noticeably, these phylogenies showed topological
493 incongruence with those of the CR/12S loci (Figures 2b, 2c). Furthermore, the four nuclear genes used
494 in these analyses did not support the existence of *RS_LinA* and *RS_LinB* lineages (Supplementary Figure
495 *S1*). The only nuclear gene that showed a similar phylogenetic pattern of that shown by the CR and 12S
496 genes, was the ITS2, which likely imply that the ITS2*,* subject to concerted evolution*,* tells a similar
497 evolutionary history to that of mitochondrial genes.
498
499 Mito-nuclear incongruence such as reported in this study have already been reported in the literature on
500 many metazoans taxa (Forsman et al., 2017; Pavlova et al., 2013; Salvi et al., 2017; Toews and
501 Brelsford, 2012; Willis et al., 2006) and they are frequently invoked as one of the main signatures of
502 selection (Morales et al., 2015), the result of incomplete lineage sorting (DeBiasse et al., 2014; Richards
503 and Hobbs, 2015; Van Oppen et al., 2001) or introgressive hybridization (Forsman et al., 2017b;

504 Gompert et al., 2008). The latter is often considered to be rampant in corals, with reticulate evolution
505 having been proposed as one of the main processes that contributed, in great extent, to their successful
506 adaptation after the geographical range expansions induced by several catastrophic events, such as the
507 Cretaceous mass extinctions and the glacial events of the Plio-Pleistocene (Veron, 1995). Our finding of
508 incongruity in the phylogenetic patterns among mitochondrial genes versus nuclear genes in *Stylophora*,
509 are therefore consistent with multiples studies in reef building corals.
510
511 In addition, to our knowledge, the degree of incongruence in mtDNA genes found in our analyses has
512 not being identified in others coral genera so far. In *Stylophora*, incongruence between the mt*ORF* and
513 the *CR* topologies was reported by Arrigoni et al. (2016) and Stefani et al. (2011).These authors
514 suggested that the most plausible hypothesis for explaining this finding was the presence of pseudogenes
515 at the mitogenome of this group, but we found no evidence for stop codons or other signs of ORF
516 disruption, rather evidence that this mt*ORF* may code for a functional transmembrane protein
517 (Banguera-Hinestroza et al. unpublished results) as proposed by Flot and Tillier (2007). Therefore, we
518 believe that other hypotheses such as recombination resulting from introgressive hybridization at the
519 mtDNA genome of *Stylophora* are equally probable as the ones discussed in Stefani et al. (2011).
520
521 In species with a uniparental inheritance of mtDNA, genes are linked and are expected to show the same
522 phylogenetic patterns (Ladoukakis and Zouros, 2017). However, contrasting topologies in mtDNA genes
523 may arise as the result of mtDNA introgressive hybridization, which is known to have a clear impact in
524 genealogical and phylogenetic reconstructions (White et al., 2008). The presence of divergent
525 mitochondrial genomes in the germline of an organism (heteroplasmy) as the result of paternal leakage
526 (Barr et al., 2005; Kuijper et al., 2015; Passamonti et al., 2013; Rokas et al., 2003) may result in mtDNA
527 recombination (considering that heteroplasmy have remained without modifications in the oocyte
528 cytoplasm long enough for allowing recombination between paternal and maternal mtDNA; White et al.,
529 2008). In the case that the recombinant genome become fixed, viable, and passed to the following
530 generations it would result in viable hybrids carrying a mixed mtDNA genome (Rokas et al., 2003;
531 White et al., 2008; Wilton et al., 2018). Even though, heteroplasmy have not been recorded in reef-
532 building corals, there is an increasing evidence that mtDNA recombination resulting from mtDNA
533 introgressive hybridization is not rare in nature (Barr et al., 2005; Levsen et al., 2016; Piganeau et al.,
534 2004; Rokas et al., 2003).

535 **4.2. mtDNA recombination explains topological incongruence**

536

537 Our recombination analyses hypothesized the *RS_LinA* as a recombinant sequence with high
538 probabilities in all methods (*P*-values ranging between 4.0 x 10^{-03} and 2.96 x 10^{-29}) with the major
539 parent being the sequence from *RS_LinB*, and only the minor parent the sequences from *S. pistillata*
540 from Taiwan. For *RS_LinA* the recombinant region –inherited from the minor parent –spans the full *nd6*,
541 *atp6* and mt*ORF* (Supplementary Figure *S3*), which explain that trees constructed with these genes
542 showed a common ancestry between the *RS_LinA* and the Indo-Pacific/Indian ocean/Madagascar
543 lineages, while the same trees show a strong diversification between these two lineages and the *RS_LinB*
544 (Figure 2 and Figure 3). Moreover, the *RS_LinA*, inherited most of its mtDNA genes from the ancestor
545 of *RS_LinB*. Therefore, it is expected that other mtDNA genes display a closest relationship between the
546 *RS_LinA* and the *RS_LinB*, as shown in our phylogenies for the CR and 12S genes and in the
547 mitogenome phylogenies excluding the recombinant region (Figure3b). Consequently, our data strongly
548 supports mtDNA introgressive hybridization followed by recombination as the main cause of mito-mito
549 topological incongruence in *Stylophora*.

550

551 We interpret these results as a strong evidence that *RS_LinA* likely arose from a hybridization event
552 between two ancestral *Stylophora* lineages. The introgression pattern follow that recorded in species of
553 hybrid zones, in which hybrids usually display an unequal mix of two mtDNA genetic backgrounds,
554 with most mitochondrial genes or genetic polymorphism passed from the genetic pool of the local
555 species to the genome of the "invader" species (asymmetric patterns of introgression; Harrison and
556 Larson, 2014).

557

558 **4.3. Interspecific phylogenies and comparative phylogeographic analyses**

559

560 As our study focuses at the population level –based on the three most variable genes used here: the
561 *hsp70*, the CR and the *mtORF* – markedly different phylogeographic patterns arises for *RS_LinA* and for
562 *RS_LinB* along the latitudinal and environmental gradient in the Red Sea (Figure 5). These patterns
563 show a strong structure for *RS_LinB*, in which the groups supported by the phylogenetic analyses
564 (Figure 4) have restricted distribution either in the northern Red Sea or in the southern Red Sea, with the
565 break between the two zones found around Yanbu, a trend that was supported by the distribution of the

566 haplotype frequencies along the gradient for each gene (Supplementary Figure *S2*). In contrast, a lack of
567 association with northern and southern environmental provinces was found in members of *RS_LinA*, and
568 rather a clinal variation in haplotype frequencies was found across the gradient (Supplementary Figure
569 *S2*).
570
571 Both lineages were also remarkably different in terms of morphology and *Symbiodinium* association: in
572 the northern Red Sea population of *RS_LinB* (i.e. subclade *LB1*; Figure 4b) most colonies were
573 associated with morphotypes of *Stylophora subseriata* (as described in Veron et al. 2018) and
574 *Symbiodinium* type C160; whereas the central-southern population (i.e. subclade LB2; Figure 4b)
575 grouped mostly individuals described in the literature as *Stylophora pistillata* and were associated
576 mainly with *Symbiodinium* type A1, but in contrast to the northern group, no colonies were found
577 carrying C160 or A1-C160 *Symbiodinium* types. Contrary to the trends detected in *RS_LinB*, colonies
578 belonging to the hybrid lineage (*RS_LinA*) showed high phenotypic plasticity and most colonies carried
579 a *Symbiodinium* type A1 in both northern and southern regions (Figure 4).
580
581 The strong differences found in both lineages, in terms of phylogeography, population subdivision, and
582 congruence/incongruence between morphology and phylogenies, reinforces the hypothesis of an early
583 colonization of the Red Sea by members of *RS_LinB* and a recent colonization of *RS_LinA* in agreement
584 with its hybrid origin. This evolutionary scenario could be explained on the light of the multiple
585 processes that have affected the region during the last glacial periods, as well as of the demographic
586 history of reef coral fauna in this region. Several studies targeting the geological dynamic of the Red Sea
587 and the patterns of diversity and endemism of its fauna (DiBattista et al., 2016a, 2016b; Fine et al.,
588 2013; Moustafa et al., 2014; Moustafa and Hallock, 2008; Rohling et al., 2008) indicate that early coral
589 reefs inhabiting this region (i.e. likely present in the region since the Miocene; Taviani 1998) were able
590 to survive extreme climatic variations in sea levels and periods of hyper salinity (Rohling et al., 2013;
591 Siddall et al., 2003; Righton et al., 1996; Rohling et al., 2013) thanks to the presence of refuge areas in
592 the northern Red Sea (i.e. the Gulf of Aqaba) and in the southern regions (i.e. Southern Red Sea and
593 Gulf of Aden) (Fine et al., 2013; Moustafa et al., 2014; Pellissier et al., 2014). Therefore, isolation in
594 these refuge zones leading to diversification and posterior recolonization may explain the differentiation
595 in allopatry of northern and central-southern populations of *RS_LinB*.

596 Furthermore, the phylogeographic patterns, such as the one presented here are also in accordance with
597 several biogeographic studies, showing that oceanographic conditions along the environmental gradient
598 of the Red Sea (Raitsos et al., 2013; Sawall et al., 2015) have originated barriers to genetic flow,
599 influenced strongly the population structure of several species, and shaped patterns of endemism in this
600 region (DiBattista et al., 2016a; Nanninga et al., 2014; Saenz-Agudelo et al., 2015), despite the fact that
601 they seem to have little impact on reef communities in terms of richness of species and species diversity
602 (Roberts et al., 2016). For example, Nanninga et al. (2013) found a good correlation between the genetic
603 differentiation among anemonefish (*Amphiprion bicinctus*) along the Saudi Arabian coast and the
604 environmental heterogeneity in this basin, with the steadiest genetic break found at approximately 19°N
605 (Southern Red Sea), which coincided with a sharp increase in turbidity in this zone. Results of our study
606 also concur with those of Froukh and Kochzius (2008, 2007) who also found high genetic differentiation
607 that were related to physical differences among fourline wrasse fish (*Larabicus quadrilineatus*) from the
608 northern and southern Red Sea. On a larger scale, research on butterfly and angel fish by Roberts et al.
609 (1992) and studies by DiBattista et al. (2013) have hypothesized that several reef fish species diversified
610 and remained restricted to the Red Sea.
611
612 **4.4. The diversification of *Stylophora* in the Red Sea and Gulf of Aden**
613
614 Our phylogeographic analyses indicate a broad distribution of *RS_LinB* across the Red Sea but limited
615 distribution in the Gulf of Aden (only few 5 out of 37 samples carrying a single mtDNA haplotypes
616 were found in this region, see also Stephani et al. 2017) (Supplementary Figure *S2*), which suggest that
617 the ancestor of *RS_LinB* was likely endemic of these regions, with the border of its distribution in the
618 Gulf of Aden. This lineage likely interbred with a lineage of broader distribution in the Indo-
619 Pacific/Indian-Ocean at the periphery of its range, which is also a confluence between several marine
620 provinces: the Red Sea and Gulf of Aden, the western Indian Ocean, and Indo-Polynesian provinces, at
621 zone that have been shown to hold several hybrid species (DiBattista et al., 2015). Moreover, the
622 phylogenetic position of Arabian Gulf haplotypes, which were placed in the same subclades of the
623 *RS_linA* specimens, implies that the hybrid expanded its range into the Arabian Gulf and into the Red
624 Sea –where it lives in sympatry with the descendants of the parental lineage–
625
626 Our results concur with multiple studies that have identified a large number of hybrid species in the Red

627 Sea (Berumen et al., 2017; DiBattista et al., 2016a) and seem to fit in the model of hybrid zones and
628 marginal areas (Barton, 1979; Hewitt, 1988), in which species from a diverse range of taxonomic groups
629 (i.e. plants, yeasts and to a lesser extent animals) living at the edge of their geographic ranges produce
630 viable hybrids carrying recombinant mitogenomes (Barr et al., 2005; Rokas et al., 2003). These hybrids
631 are able to adapt to new climatic conditions, and diverge in sympatric association with their parental
632 species (Ballard and Whitlock, 2004; Barr et al., 2005; Fourie et al., 2018; Galtier, 2011; Leducq et al.,
633 2017; Mastrantonio et al., 2016; Peris et al., 2017; Rokas et al., 2003; Ujvari et al., 2007). Moreover, the
634 pattern found in our results in *Stylophora* were similar to those found in hybrid species of marine reef-
635 fishes, found at the intersection of three main biogeographical regions: the Red Sea and Gulf of Aden,
636 the western Indian Ocean and the Indo-Polynesian provinces (DiBattista et al., 2015). These authors
637 identify 14 hybrid species based in molecular markers and morphological characteristics, the gene flow
638 was unidirectional, and the parental species were found at the periphery of their distribution range,
639 where they showed the lowest abundance. Interestingly, as in our work with *Stylophora*, the reported
640 hybrids were found to be the result of intercrosses between endemic species, with restricted distribution
641 range in the Red Sea and Arabian Gulf, with species broadly distributed in the Indo-Pacific, and the
642 major parental species was at the limit of its distribution and almost absent from the Gulf of Aden area.
643
644 **4.5. Implications for conservation in a climate change scenario**
645
646 Under the current challenges that climatic change poses for coral reef ecosystems, particularly with the
647 rising of oceanic temperatures above the limit threshold of most species (1°C above mean summer
648 maximum) (Hughes et al., 2018; Pandolfi et al., 2011) evolutionary studies with a clear assessment of the
649 demographic history of species and populations are of great relevance, particularly to understand the main
650 mechanisms involved in adaptation and speciation in variable and extreme environments. Our study,
651 coupling recombination analyses, phylogenetic and phylogeographic patterns, suggest that mtDNA genes
652 may play a key role in adaptation to extreme environments in coral species.
653
654 Two genes, the *atp6* gene and the mt*ORF* gene showed high mutation rates and extreme variability in
655 the *RS_LinB* leading to amino acid and structural changes in their encoded proteins, particularly in the
656 mt*ORF* (Banguera-Hinestroza et al. unpublished data). Interestingly, the *atp6* gene is part of a group of
657 genes that are essential in releasing and controlling the proliferation of deleterious oxygen radicals

658 (ROS) in the mitochondria (Kühlbrandt., 2015; Wirth et al., 2016), which are known for causing
659 oxidative damage to symbionts and corals during exposition to high temperatures, with the subsequent
660 bleaching and dead of corals (Downs et al., 2002; Smith et al., 2005).
661
662 In *RS_LinB*, the frequencies of the most common haplotypes of the mt*ORF* locus were associated with
663 coldest (north) or hottest (central-south) areas in the Red Sea (Supplementary Figure S2), a tendency
664 that was also followed by the haplotype frequencies of the *hsp70* gene –a chaperone protein involved in
665 heat stress response (Kvitt et al., 2016; Mayer and Bukau, 2005)–, suggesting that both proteins may
666 have played a similar role in the adaptation to temperature in *RS_LinB* variants. This premise was
667 supported by the computational characterization of the mt*ORF* protein (Banguera-Hinestroza et al.
668 unpublished) in which searches against approx. 95 million protein domains classified in the CATH data
669 base –using the pDomTHREADER approach (Lobley et al., 2009)–, revealed that domains in the
670 mt*ORF* protein of *RS_LinB*, have the highest matches with annotated domains involved in the structural
671 integrity of a complex or its assembly within or outside a cell (CATH domain code: 1s58A00) and
672 domains that play a role in cell-to-cell, cell-to-matrix interactions, and response to stress (1ux6A01) with
673 high levels of confidence ($0.001 < P < 0.01$).
674
675 These findings may suggest that selective pressures imposed by the extreme environmental variations in
676 the Red Sea along multiple geological periods, may had have an impact in the mitogenome of this
677 lineage, with consequences in adaptation and speciation, as have been found in other taxa evolving in a
678 broad range of environmental conditions (Hill, 2017, 2016; Lamb et al., 2018). Even though the
679 *RS_LinB* hybridized with an Indo-Pacific/Indian Ocean lineage, the resulting hybrid (*RS_LinA*) did not
680 inherited the variation at the *nd6*, *atp6* and mt*ORF* genes, this open the question whether other
681 mitochondrial genes or mtDNA mechanisms may play a role in hybrid speciation and adaptation, or
682 whether the hybrid may be more vulnerable to strong temperature variation (i.e. nowadays the *RS_LinA*
683 is very rare in the Arabian Gulf Area; Banguera-Hinestroza et al. unpublished results).
684
685 Taken together, our data indicate that hybridization in corals could be more complex than commonly
686 expected, involving mechanisms such as mitochondrial metabolism and mitochondrial genome
687 evolution as have been previoulsy emphasized by Dixon et al., (2015) that demonstrated a strong
688 maternal effect in heat stress tolerance. Assisted hybridization has been proposed as an alternative for

conservation of coral reef via genetic rescue (Chan et al., 2018); however, little is known about the molecular mechanisms enhancing hybrid adaptation and speciation under extreme climatic conditions. A clear understanding of these mechanisms coupled with the demographic history of coral populations is therefore needed to pursue effective conservation plans.

Funding statement

This research was funded by King Abdullah University of Science and Technology (KAUST), Saudi Arabia (sample analysis) and by King Abdulaziz University (KAU) as part of the Jeddah Transect project (sample collection) and by a postdoctoral research fellowship from the Université libre de Bruxelles, Belgium.

Acknowledgments: The authors want to thank Dr. Veron for assistance with voucher identification, Dr. Saenz Agudelo for sample collections and recommendations, Dr. Bouwmeester for sample collection, Vanessa Robitzch for helping with the DNA extractions, Catalina Ramirez for her support in bioinformatics pipelines and Sebastien Santini - CNRS/AMU IGS UMR7256, for its effort in maintaining the excellence of the Phylogeny.fr site. We thanks to King Abdulaziz University (KAU) and the Bioscience Core Lab at KAUST for sharing their facilities.

5. REFERENCES

Acker, J., Leptoukh, G., Shen, S., Zhu, T., Kempler, S., 2008. Remotely-sensed chlorophylla observations of the northern Red Sea indicate seasonal variability and influence of coastal reefs. J. Mar. Syst. 69, 191–204. https://doi.org/10.1016/j.jmarsys.2005.12.006

Al Arab, M., Höner zu Siederdissen, C., Tout, K., Sahyoun, A.H., Stadler, P.F., Bernt, M., 2017. Accurate annotation of protein-coding genes in mitochondrial genomes. Mol. Phylogenet. Evol. 106, 209–216. https://doi.org/10.1016/j.ympev.2016.09.024

Anisimova, M., Gascuel, O., 2006. Approximate Likelihood-Ratio test for branches: A fast, accurate, and powerful alternative. Syst. Biol. 55, 539–552. https://doi.org/10.1080/10635150600755453

Arrigoni, R., Benzoni, F., Terraneo, T.I., Caragnano, A., Berumen, M.L., 2016. Recent origin and semi-permeable species boundaries in the scleractinian coral genus *Stylophora* from the Red Sea. Sci. Rep. 6, 34612. https://doi.org/10.1038/srep34612

720 Ballard, J.W.O., Rand, D.M., 2005. The population biology of mitochondrial DNA and its phylogenetic
721 implications. Annu. Rev. Ecol. Evol. Syst. 36, 621–642.
722 https://doi.org/10.1146/annurev.ecolsys.36.091704.175513
723 Ballard, J.W.O., Whitlock, M.C., 2004. The incomplete natural history of mitochondria. Mol. Ecol. 13,
724 729–744. https://doi.org/10.1046/j.1365-294X.2003.02063.x
725 Barr, C.M., Neiman, M., Taylor, D.R., 2005. Inheritance and recombination of mitochondrial genomes
726 in plants, fungi and animals. New Phytol. 168, 39–50. https://doi.org/10.1111/j.1469-
727 8137.2005.01492.x
728 Barton, N.H., 1979. The dynamics of hybrid zones. Heredity (Edinb). 43, 341–359.
729 https://doi.org/10.1038/hdy.1979.87
730 Bernt, M., Donath, A., Jühling, F., Externbrink, F., Florentz, C., Fritzsch, G., Pütz, J., Middendorf, M.,
731 Stadler, P.F., 2013. MITOS: Improved de novo metazoan mitochondrial genome annotation. Mol.
732 Phylogenet. Evol. 69, 313–319. https://doi.org/10.1016/j.ympev.2012.08.023
733 Berumen, M.L., DiBattista, J.D., Rocha, L.A., 2017. Introduction to virtual issue on Red Sea and
734 Western Indian Ocean biogeography. J. Biogeogr. 44, 1923–1926.
735 https://doi.org/10.1111/jbi.13036
736 Boni, M.F., Posada, D., Feldman, M.W., 2006. An exact nonparametric method for inferring mosaic
737 structure in sequence triplets. Genetics 176, 1035–1047.
738 https://doi.org/10.1534/genetics.106.068874
739 Brennan, A.C., Woodward, G., Seehausen, O., Muñoz-Fuentes, V., Moritz, C., Guelmami, A., Abbott,
740 R.J., Edelaar, P., 2014. Hybridization due to changing species distributions: Adding problems or
741 solutions to conservation of biodiversity during global change? Evol. Ecol. Res. 16, 475–491.
742 Chan, W.Y., Peplow, L.M., Menéndez, P., Hoffmann, A.A., van Oppen, M.J.H., 2018. Interspecific
743 hybridization may provide novel opportunities for coral reef restoration. Front. Mar. Sci. 5, 1–15.
744 https://doi.org/10.3389/fmars.2018.00160
745 Chen, C., Chiou, C.-Y., Dai, C.-F., Chen, C.A., 2008. Unique mitogenomic features in the scleractinian
746 family pocilloporidae (Scleractinia: Astrocoeniina). Mar. Biotechnol. 10, 538–553.
747 https://doi.org/10.1007/s10126-008-9093-x
748 Chinnery, P.F., Hudson, G., 2013. Mitochondrial genetics. Br. Med. Bull. 106, 135–159.
749 https://doi.org/10.1093/bmb/ldt017
750 Combosch, D.J., Vollmer, S. V, 2015. Trans-Pacific RAD-Seq population genomics confirms

751 introgressive hybridization in Eastern Pacific *Pocillopora* corals. Mol. Phylogenet. Evol. 88, 154–
752 162. https://doi.org/10.1016/j.ympev.2015.03.022
753 DeBiasse, M.B., Nelson, B.J., Hellberg, M.E., 2014. Evaluating summary statistics used to test for
754 incomplete lineage sorting: mito-nuclear discordance in the reef sponge *Callyspongia vaginalis*.
755 Mol. Ecol. 23, 225–238. https://doi.org/10.1111/mec.12584
756 Dereeper, A., Audic, S., Claverie, J.M.M., Blanc, G., 2010. BLAST-EXPLORER helps you building
757 datasets for phylogenetic analysis. BMC Evol. Biol. 10, 8. https://doi.org/10.1186/1471-2148-10-8
758 Dereeper, A., Guignon, V., Blanc, G., Audic, S., Buffet, S., Chevenet, F., Dufayard, J.F., Guindon, S.,
759 Lefort, V., Lescot, M., Claverie, J.M., Gascuel, O., 2008. Phylogeny.fr: robust phylogenetic
760 analysis for the non-specialist. Nucleic Acids Res. 36, W465–W469.
761 https://doi.org/10.1093/nar/gkn180
762 DiBattista, J.D., Berumen, M.L., Gaither, M.R., Rocha, L.A., Eble, J.A., Choat, J.H., Craig, M.T.,
763 Skillings, D.J., Bowen, B.W., 2013. After continents divide: comparative phylogeography of reef
764 fishes from the Red Sea and Indian Ocean. J. Biogeogr. 40, 1170–1181.
765 https://doi.org/10.1111/jbi.12068
766 DiBattista, J.D., Howard Choat, J., Gaither, M.R., Hobbs, J.P.A., Lozano-Cortés, D.F., Myers, R.F.,
767 Paulay, G., Rocha, L.A., Toonen, R.J., Westneat, M.W., Berumen, M.L., 2016a. On the origin of
768 endemic species in the Red Sea. J. Biogeogr. 43, 13–30. https://doi.org/10.1111/jbi.12631
769 DiBattista, J.D., Roberts, M.B., Bouwmeester, J., Bowen, B.W., Coker, D.J., Lozano-Cortés, D.F.,
770 Howard Choat, J., Gaither, M.R., Hobbs, J.P.A., Khalil, M.T., Kochzius, M., Myers, R.F., Paulay,
771 G., Robitzch, V.S.N., Saenz-Agudelo, P., Salas, E., Sinclair-Taylor, T.H., Toonen, R.J., Westneat,
772 M.W., Williams, S.T., Berumen, M.L., 2016b. A review of contemporary patterns of endemism for
773 shallow water reef fauna in the Red Sea. J. Biogeogr. 43, 423–439.
774 https://doi.org/10.1111/jbi.12649
775 DiBattista, J.D., Rocha, L.A., Hobbs, J.-P.A., He, S., Priest, M.A., Sinclair-Taylor, T.H., Bowen, B.W.,
776 Berumen, M.L., 2015. When biogeographical provinces collide: hybridization of reef fishes at the
777 crossroads of marine biogeographical provinces in the Arabian Sea. J. Biogeogr. 42, 1601–1614.
778 https://doi.org/10.1111/jbi.12526
779 Diekmann, O. E., Bak, R. P. M., Stam, W. T., & Olsen, J. L. 2001. Molecular genetic evidence for
780 probable reticulate speciation in the coral genus *Madracis* from a Caribbean fringing reef slope.
781 Mar. Biol. 139, 221–233. https://doi.org/10.1007/s002270100584

Dierckxsens, N., Mardulyn, P., Smits, G., 2016. NOVOPlasty: de novo assembly of organelle genomes from whole genome data. Nucleic Acids Res. 45, gkw955. https://doi.org/10.1093/nar/gkw955

Dixon, G.B., Davies, S.W., Aglyamova, G. V., Meyer, E., Bay, L.K., Matz, M. V., 2015. Genomic determinants of coral heat tolerance across latitudes. Science. 348, 1460–1462. https://doi.org/10.1126/science.1261224

Dokianakis, E., Ladoukakis, E.D., 2014. Different degree of paternal mtDNA leakage between male and female progeny in interspecific *Drosophila* crosses. Ecol. Evol. 4, 2633–2641. https://doi.org/10.1002/ece3.1069

Downs, C.A., Fauth, J.E., Halas, J.C., Dustan, P., Bemiss, J., Woodley, C.M., 2002. Oxidative stress and seasonl coral bleaching. Free Radic. Biol. Med. 33, 533–543.

Edgar, R.C., 2004. MUSCLE: multiple sequence alignment with high accuracy and high throughput. Nucleic Acids Research. 32, 1792–1797. https://doi.org/10.1093/nar/gkh340

Ehrenberg, C.G., 1834. Die Corallenthiere des Rothen Meeres physiologisch untersucht un systematisch verzeichnet. gedruckt in der Druckerei der K. Akademie der Wissenschafte, Berlin (156)

Esper, E.J.C., 1797. Fortsetzungen der Pflanzenthiere in Abbildungen nach der Natur mit Farben erleuchtet nebst Beschreibungen. Erster Theil. Raspische Buchhandlung, Nürnberg.

Excoffier, L., Lischer, H.E.L., 2010. Arlequin suite ver 3.5: A new series of programs to perform population genetics analyses under Linux and Windows. Mol. Ecol. Resour. 10, 564–567. https://doi.org/10.1111/j.1755-0998.2010.02847.x

Fine, M., Gildor, H., Genin, A., 2013. A coral reef refuge in the Red Sea. Glob. Chang. Biol. 19, 3640–3647. https://doi.org/10.1111/gcb.12356

Flot, J.F., 2010. seqphase: a web tool for interconverting phase input/output files and fasta sequence alignments. Mol. Ecol. Resour. 10, 162–166. https://doi.org/10.1111/j.1755-0998.2009.02732.x

Flot, J.F., Blanchot, J., Charpy, L., Cruaud, C., Licuanan, W.Y., Nakano, Y., Payri, C., Tillier, S., 2011. Incongruence between morphotypes and genetically delimited species in the coral genus *Stylophora*: phenotypic plasticity, morphological convergence, morphological stasis or interspecific hybridization? BMC Ecol. 11, 22. https://doi.org/10.1186/1472-6785-11-22

Flot, J.F., Tillier, S., 2007. The mitochondrial genome of *Pocillopora* (Cnidaria: Scleractinia) contains two variable regions: The putative D-loop and a novel ORF of unknown function. Gene 401, 80–87. https://doi.org/10.1016/j.gene.2007.07.006

Flot J.F., 2007. Towards a molecular taxonomy of corals of the genus *Pocillopora*. Ph.D. thesis,

(Muséum national d'Histoire naturelle, Paris).
Flot, J.F., Tillier, A., Samadi, S., Tillier, S., 2006. Phase determination from direct sequencing of length-variable DNA regions. Mol. Ecol. Notes. https://doi.org/10.1111/j.1471-8286.2006.01355.x
Forsman, Z.H., Knapp, I.S.S., Tisthammer, K., Eaton, D.A.R., Belcaid, M., Toonen, R.J., 2017. Coral hybridization or phenotypic variation? Genomic data reveal gene flow between *Porites lobata* and *P. Compressa*. Mol. Phylogenet. Evol. 111, 132–148. https://doi.org/10.1016/j.ympev.2017.03.023
Fourie, G., Van der Merwe, N.A., Wingfield, B.D., Bogale, M., Wingfield, M.J., Steenkamp, E.T., 2018. Mitochondrial introgression and interspecies recombination in the *Fusarium fujikuroi* species complex. IMA Fungus 9, 37–63. https://doi.org/10.5598/imafungus.2018.09.01.04
Froukh, T., Kochzius, M., 2008. Species boundaries and evolutionary lineages in the blue green damselfishes *Chromis viridis* and *Chromis atripectoralis* (Pomacentridae). J. Fish Biol. 72, 451–457. https://doi.org/10.1111/j.1095-8649.2007.01746.x
Froukh, T., Kochzius, M., 2007. Genetic population structure of the endemic fourline wrasse (*Larabicus quadrilineatus*) suggests limited larval dispersal distances in the Red Sea. Mol. Ecol. 16, 1359–1367. https://doi.org/10.1111/j.1365-294X.2007.03236.x
Gaither, M.R., Szabó, Z., Crepeau, M.W., Bird, C.E., Toonen, R.J., 2011. Preservation of corals in salt-saturated DMSO buffer is superior to ethanol for PCR experiments. Coral Reefs 30, 329–333. https://doi.org/10.1007/s00338-010-0687-1
Galtier, N., 2011. The intriguing evolutionary dynamics of plant mitochondrial DNA. BMC Biol. 9, 61. https://doi.org/10.1186/1741-7007-9-61
Garzón-Ospina, D., López, C., Forero-Rodríguez, J., Patarroyo, M.A., 2012. Genetic Diversity and Selection in Three *Plasmodium vivax* Merozoite Surface Protein 7 (Pvmsp-7) Genes in a Colombian Population. PLoS One 7, e45962. https://doi.org/10.1371/journal.pone.0045962
Gibbs, M.J., Armstrong, J.S., Gibbs, A.J., 2000. Sister-Scanning: a Monte Carlo procedure for assessing signals in recombinant sequences. Bioinformatics 16, 573–582. https://doi.org/10.1093/bioinformatics/16.7.573
Gompert, Z., Forister, M.L., Fordyce, J.A., Nice, C.C., 2008. Widespread mito-nuclear discordance with evidence for introgressive hybridization and selective sweeps in Lycaeides. Mol. Ecol. 17, 5231–5244. https://doi.org/10.1111/j.1365-294X.2008.03988.x
Guindon, S., Dufayard, J.-F., Lefort, V., Anisimova, M., Hordijk, W., Gascuel, O., 2010. New algorithms and methods to estimate Maximum-Likelihood phylogenies: Asessing the performance

844 of PhyML 2.0. Syst. Biol. https://doi.org/10.1093/sysbio/syq010
845 Harrison, R.G., Larson, E.L., 2014. Hybridization, Introgression, and the nature of species boundaries. J.
846 Hered. 105, 795–809. https://doi.org/10.1093/jhered/esu033
847 Hellberg, M.E., Prada, C., Tan, M.H., Forsman, Z.H., Baums, I.B., 2016. Getting a grip at the edge:
848 recolonization and introgression in eastern Pacific *Porites* corals. J. Biogeogr. 43, 2147–2159.
849 https://doi.org/10.1111/jbi.12792
850 Hewitt, G.M., 1988. Hybrid zones-natural laboratories for evolutionary studies. Trends Ecol. Evol. 3,
851 158–167. https://doi.org/10.1016/0169-5347(88)90033-X
852 Hill, G.E., 2017. The mitonuclear compatibility species concept. Auk 134, 393–409.
853 https://doi.org/10.1642/AUK-16-201.1
854 Hill, G.E., 2016. Mitonuclear coevolution as the genesis of speciation and the mitochondrial DNA
855 barcode gap. Ecol. Evol. 6, 5831–5842. https://doi.org/10.1002/ece3.2338
856 Huelsenbeck, J.P., Ronquist, F., 2001. Mr. BAYES: Bayesian inference of phylogenetic trees.
857 Bioinformatics 17, 754–755. https://doi.org/10.1093/bioinformatics/17.8.754
858 Hughes, T.P., Kerry, J.T., Baird, A.H., Connolly, S.R., Dietzel, A., Eakin, C.M., Heron, S.F., Hoey,
859 A.S., Hoogenboom, M.O., Liu, G., McWilliam, M.J., Pears, R.J., Pratchett, M.S., Skirving, W.J.,
860 Stella, J.S., Torda, G., 2018. Global warming transforms coral reef assemblages. Nature 556, 492–
861 496. https://doi.org/10.1038/s41586-018-0041-2
862 Johannesson, K., Carl, A., 2006. Life on the margin: genetic isolation and diversity loss in a peripheral
863 marine ecosystem, the Baltic Sea. Mol. Ecol. 15, 2013–2029. https://doi.org/10.1111/j.1365-
864 294X.2006.02919.x
865 Johnston, E.C., Forsman, Z.H., Flot, J.-F., Schmidt-Roach, S., Pinzón, J.H., Knapp, I.S.S., Toonen, R.J.,
866 2017. A genomic glance through the fog of plasticity and diversification in *Pocillopora*. Sci. Rep.
867 7, 5991. https://doi.org/10.1038/s41598-017-06085-3
868 Katoh, K., Standley, D.M., 2013. MAFFT Multiple Sequence Alignment Software Version 7:
869 Improvements in Performance and Usability. Mol. Biol. Evol. 30, 772–780.
870 https://doi.org/10.1093/molbev/mst010
871 Keshavmurthy, S., Yang, S.-Y., Alamaru, A., Chuang, Y.-Y., Pichon, M., Obura, D., Fontana, S., De
872 Palmas, S., Stefani, F., Benzoni, F., MacDonald, A., Noreen, A.M.E., Chen, C., Wallace, C.C.,
873 Pillay, R.M., Denis, V., Amri, A.Y., Reimer, J.D., Mezaki, T., Sheppard, C., Loya, Y., Abelson, A.,
874 Mohammed, M.S., Baker, A.C., Mostafavi, P.G., Suharsono, B.A., Chen, C.A., 2013. DNA

875 barcoding reveals the coral “laboratory-rat”, *Stylophora pistillata* encompasses multiple identities.
876 Sci. Rep. 3, 1520. https://doi.org/10.1038/srep01520
877 Kivisild, T., 2015. Maternal ancestry and population history from whole mitochondrial genomes.
878 Investig. Genet. 6, 3. https://doi.org/10.1186/s13323-015-0022-2
879 Klueter, A., Andreakis, N., 2013. Assessing genetic diversity in the scleractinian coral *Stylophora*
880 *pistillata* (Esper 1797) from the Central Great Barrier Reef and the Coral Sea. Syst. Biodivers. 11,
881 67–76. https://doi.org/10.1080/14772000.2013.770419
882 Kühlbrandt, W., 2015. Structure and function of mitochondrial membrane protein complexes. BMC
883 Biol. 13, 89. https://doi.org/10.1186/s12915-015-0201-x
884 Kuijper, B., Lane, N., Pomiankowski, A., 2015. Can paternal leakage maintain sexually antagonistic
885 polymorphism in the cytoplasm? J. Evol. Biol. 28, 468–480. https://doi.org/10.1111/jeb.12582
886 Kumar, S., Stecher, G., Tamura, K., 2016. MEGA7: Molecular Evolutionary Genetics Analysis Version
887 7.0 for Bigger Datasets. Mol. Biol. Evol. 33, 1870–1874. https://doi.org/10.1093/molbev/msw054
888 Kvitt, H., Rosenfeld, H., Tchernov, D., 2016. The regulation of thermal stress induced apoptosis in
889 corals reveals high similarities in gene expression and function to higher animals. Sci. Rep. 6,
890 30359. https://doi.org/10.1038/srep30359
891 Ladoukakis, E.D., Zouros, E., 2017. Evolution and inheritance of animal mitochondrial DNA: Rules and
892 exceptions. J. Biol. Res. 24, 1–7. https://doi.org/10.1186/s40709-017-0060-4
893 Lamb, A.M., Gan, H.M., Greening, C., Joseph, L., Lee, Y.P., Morán-Ordóñez, A., Sunnucks, P.,
894 Pavlova, A., 2018. Climate-driven mitochondrial selection: A test in Australian songbirds. Mol.
895 Ecol. 27, 898–918. https://doi.org/10.1111/mec.14488
896 Leducq, J.-B., Henault, M., Charron, G., Nielly-Thibault, L., Terrat, Y., Fiumera, H.L., Shapiro, B.J.,
897 Landry, C.R., 2017. Mitochondrial recombination and introgression during speciation by
898 Hybridization. Mol. Biol. Evol. 34, 1947–1959. https://doi.org/10.1093/molbev/msx139
899 Levsen, N., Bergero, R., Charlesworth, D., Wolff, K., 2016. Frequent, geographically structured
900 heteroplasmy in the mitochondria of a flowering plant, ribwort plantain (*Plantago lanceolata*).
901 Heredity (Edinb). 117, 1–7. https://doi.org/10.1038/hdy.2016.15
902 Librado, P., Rozas, J., 2009. DnaSP v5: A software for comprehensive analysis of DNA polymorphism
903 data. Bioinformatics 25, 1451–1452. https://doi.org/10.1093/bioinformatics/btp187
904 Lobley, A., Sadowski, M.I., Jones, D.T., 2009. pGenTHREADER and pDomTHREADER: new
905 methods for improved protein fold recognition and superfamily discrimination. Bioinformatics 25,

906 1761–1767. https://doi.org/10.1093/bioinformatics/btp302
907 Martin, D.P., Lemey, P., Lott, M., Moulton, V., Posada, D., Lefeuvre, P., 2010. RDP3: A flexible and
908 fast computer program for analyzing recombination. Bioinformatics 26, 2462–2463.
909 https://doi.org/10.1093/bioinformatics/btq467
910 Martin, D.P., Murrell, B., Golden, M., Khoosal, A., Muhire, B., 2015. RDP4: Detection and analysis of
911 recombination patterns in virus genomes. Virus Evol. 1, vev003. https://doi.org/10.1093/ve/vev003
912 Martin, D.P., Posada, D., Crandall, K.A., Williamson, C., 2005. A modified Bootscan algorithm for
913 automated identification of recombinant sequences and recombination breakpoints. AIDS Res.
914 Hum. Retroviruses 21, 98–102. https://doi.org/10.1089/aid.2005.21.98
915 Mastrantonio, V., Porretta, D., Urbanelli, S., Crasta, G., Nascetti, G., 2016. Dynamics of mtDNA
916 introgression during species range expansion: insights from an experimental longitudinal study.
917 Sci. Rep. 6, 30355. https://doi.org/10.1038/srep30355
918 Mayer, M.P., Bukau, B., 2005. Hsp70 chaperones: Cellular functions and molecular mechanism. Cell.
919 Mol. Life Sci. 62, 670–684. https://doi.org/10.1007/s00018-004-4464-6
920 Miller, M.A., Pfeiffer, W., Schwartz, T., 2010. Creating the CIPRES Science Gateway for inference of
921 large phylogenetic trees, in: 2010 Gateway Computing Environments Workshop (GCE). IEEE, pp.
922 1–8. https://doi.org/10.1109/GCE.2010.5676129
923 Morales, H.E., Pavlova, A., Joseph, L., Sunnucks, P., 2015. Positive and purifying selection in
924 mitochondrial genomes of a bird with mitonuclear discordance. Mol. Ecol. 24, 2820–37.
925 https://doi.org/10.1111/mec.13203
926 Moustafa, M.Z., Hallock, P., 2008. Observations of a Red Sea Fringing Coral Reef under Extreme
927 Environmental Conditions. 11th Int. Coral Reef Symp. Ft. Lauderdale, Florida 7–11.
928 Moustafa, M.Z., Moustafa, M.S., Moustafa, Z.D., Moustafa, S.E., 2014. Survival of high latitude
929 fringing corals in extreme temperatures: Red Sea oceanography. J. Sea Res. 88, 144–151.
930 https://doi.org/10.1016/j.seares.2014.01.012
931 Nanninga, G.B., Saenz-Agudelo, P., Manica, A., Berumen, M.L., 2014. Environmental gradients predict
932 the genetic population structure of a coral reef fish in the Red Sea. Mol. Ecol. 23, 591–602.
933 https://doi.org/10.1111/mec.12623
934 Padidam, M., Sawyer, S., Fauquet, C.M., 1999. Possible emergence of new gemini viruses by frequent
935 recombination. Virology 265, 218–225. https://doi.org/10.1006/viro.1999.0056
936 Pandolfi, J.M., Connolly, S.R., Marshall, D.J., Cohen, A.L., 2011. Projecting coral reef futures under

937 global warming and ocean acidification. Science. 333, 418–422.
938 https://doi.org/10.1126/science.1204794
939 Passamonti, M., Ghiselli, F., Milani, L., 2013. Mitochondrial Inheritance, in: Brenner's Encyclopedia of
940 Genetics. Elsevier, pp. 443–445. https://doi.org/10.1016/B978-0-12-374984-0.00960-8
941 Pavlova, A., Amos, J.N., Joseph, L., Loynes, K., Austin, J.J., Keogh, J.S., Stone, G.N., Nicholls, J.A.,
942 Sunnucks, P., 2013. Perched at the mito-nuclear crossroads: divergent mitochondrial lineages
943 correlate with environment in the face of ongoing nuclear gene flow in an australian bird.
944 Evolution. 67, 3412–3428. https://doi.org/10.1111/evo.12107
945 Pellissier, L., Leprieur, F., Parravicini, V., Cowman, P.F., Kulbicki, M., Litsios, G., Olsen, S.M., Wisz,
946 M.S., Bellwood, D.R., Mouillot, D., 2014. Quaternary coral reef refugia preserved fish diversity.
947 Science. 344, 1016–1019. https://doi.org/10.1126/science.1249853
948 Peris, D., Arias, A., Orlić, S., Belloch, C., Pérez-Través, L., Querol, A., Barrio, E., 2017. Mitochondrial
949 introgression suggests extensive ancestral hybridization events among *Saccharomyces* species.
950 Mol. Phylogenet. Evol. 108, 49–60. https://doi.org/10.1016/j.ympev.2017.02.008
951 Piganeau, G., Gardner, M., Eyre-Walker, A., 2004. A broad survey of recombination in animal
952 mitochondria. Mol. Biol. Evol. https://doi.org/10.1093/molbev/msh244
953 Posada, D., Crandall, K.A., 2001. Evaluation of methods for detecting recombination from DNA
954 sequences: Computer simulations. Proc. Natl. Acad. Sci. 98, 13757–13762.
955 https://doi.org/10.1073/pnas.241370698
956 Raitsos, D.E., Pradhan, Y., Brewin, R.J.W., Stenchikov, G., Hoteit, I., 2013. Remote Sensing the
957 Phytoplankton Seasonal Succession of the Red Sea. PLoS One 8, e64909.
958 https://doi.org/10.1371/journal.pone.0064909
959 Rambaut, A., Drummond, A.J., 2009. Tracer v 1.5. http://beast.bio.ed.ac.uk/Tracer.
960 Richards, Z.T., Hobbs, J.P.A., 2015. Hybridisation on coral reefs and the conservation of evolutionary
961 novelty. Curr. Zool. 61, 132–145. https://doi.org/10.1093/czoolo/61.1.132
962 Righton, D., Kemp, J., Ormond, R., 1996. Biogeography community structure and diversity of Red Sea
963 and western Indian Ocean butterflyfishes. J. Mar. Biol. Assoc. United Kingdom 76, 223–228.
964 Riginos, C., Cunningham, C.W., 2004. Invited Review: Local adaptation and species segregation in two
965 mussel (*Mytilus edulis* × *Mytilus trossulus*) hybrid zones. Mol. Ecol. 14, 381–400.
966 https://doi.org/10.1111/j.1365-294X.2004.02379.x
967 Roberts, M.B., Jones, G.P., McCormick, M.I., Munday, P.L., Neale, S., Thorrold, S., Robitzch, V.S.N.,

968 Berumen, M.L., 2016. Homogeneity of coral reef communities across 8 degrees of latitude in the
969 Saudi Arabian Red Sea. Mar. Pollut. Bull. 105, 558–565.
970 https://doi.org/10.1016/j.marpolbul.2015.11.024
971 Rohling, E.J., Grant, K., Hemleben, C., Siddall, M., Hoogakker, B.A.A., Bolshaw, M., Kucera, M.,
972 2008. High rates of sea-level rise during the last interglacial period. Nat. Geosci. 1, 38–42.
973 https://doi.org/10.1038/ngeo.2007.28
974 Rohling, E.J., Grant, K.M., Roberts, A.P., Larrasoaña, J.-C., 2013. Paleoclimate variability in the
975 mediterranean and red sea regions during the last 500,000 years. Curr. Anthropol. 54, S183–S201.
976 https://doi.org/10.1086/673882
977 Rokas, A., Ladoukakis, E., Zouros, E., 2003. Animal mitochondrial DNA recombination revisited.
978 Trends Ecol. Evol. 18, 411–417. https://doi.org/10.1016/S0169-5347(03)00125-3
979 Saenz-Agudelo, P., Dibattista, J.D., Piatek, M.J., Gaither, M.R., Harrison, H.B., Nanninga, G.B.,
980 Berumen, M.L., 2015. Seascape genetics along environmental gradients in the Arabian Peninsula:
981 insights from ddRAD sequencing of anemonefishes. Mol. Ecol. 24, 6241–6255.
982 https://doi.org/10.1111/mec.13471
983 Salvi, D., Pinho, C., Harris, D.J., 2017. Digging up the roots of an insular hotspot of genetic diversity:
984 Decoupled mito-nuclear histories in the evolution of the Corsican-Sardinian endemic lizard
985 *Podarcis tiliguerta*. BMC Evol. Biol. 17. https://doi.org/10.1186/s12862-017-0899-x
986 Sawall, Y., Al-Sofyani, A., Banguera-Hinestroza, E., Voolstra, C.R., 2014. Spatio-temporal analyses of
987 *symbiodinium* physiology of the coral *Pocillopora verrucosa* along large-scale nutrient and
988 temperature gradients in the Red Sea. PLoS One 9, e103179.
989 https://doi.org/10.1371/journal.pone.0103179
990 Sawall, Y., Al-Sofyani, A., Hohn, S., Banguera-Hinestroza, E., Voolstra, C.R., Wahl, M., 2015.
991 Extensive phenotypic plasticity of a Red Sea coral over a strong latitudinal temperature gradient
992 suggests limited acclimatization potential to warming. Sci. Rep. 5, 8940.
993 https://doi.org/10.1038/srep08940
994 Scheer, G., Pillai, C.S.G., 1983. Report on the stony corals from the Red Sea. Zoologica 131, 1–198.
995 Seutin, G., White, B.N., Boag, P.., 1991. Preservation of avian blood and tissue samples for DNA
996 analyses. Can. J. Zool. 69, 89–90.
997 Shearer, T.L., Oppen, M.J.H. Van, Romano, S.L., G. Worheire, 2002. Slow mitochondria DNA
998 sequence evolution in the Anthozoa. Mol. Ecol. 11, 2475–2487.

Siddall, M., Rohling, E.J., Almogi-Labin, A., Hemleben, C., Meischner, D., Schmelzer, I., Smeed, D. a, 2003. Sea-level fluctuations during the last glacial cycle. Nature 423, 853–858. https://doi.org/10.1038/nature01690

Siddall, M., Smeed, D.A., Hemleben, C., Rohling, E.J., Schmelzer, I., Peltier, W.R., 2004. Understanding the Red Sea response to sea level. Earth Planet. Sci. Lett. 225, 421–434. https://doi.org/DOI 10.1016/j.epsl.2004.06.008

Smith, D.J., Suggett, D.J., Baker, N.R., 2005. Is photoinhibition of zooxanthellae photosynthesis the primary cause of thermal bleaching in corals? Glob. Chang. Biol. 11, 1–11. https://doi.org/10.1111/j.1529-8817.2003.00895.x

Smith, J., 1992. Analyzing the mosaic structure of genes. J. Mol. Evol. 34. https://doi.org/10.1007/BF00182389

Stefani, F., Benzoni, F., Yang, S.-Y., Pichon, M., Galli, P., Chen, C.A., 2011. Comparison of morphological and genetic analyses reveals cryptic divergence and morphological plasticity in *Stylophora* (Cnidaria, Scleractinia). Coral Reefs 30, 1033–1049. https://doi.org/10.1007/s00338-011-0797-4

Stephens, M., Donnelly, P., 2003. A Comparison of bayesian methods for haplotype reconstruction from population genotype data. Am. J. Hum. Genet. 73, 1162–1169. https://doi.org/10.1086/379378

Taviani, M., 1998. Post-Miocene reef faunas of the Red Sea: glacio-eustatic controls, in: Sedimentation and tectonics in rift basins Red Sea-Gulf of Aden. Springer Netherlands, Dordrecht, pp. 574–582. https://doi.org/10.1007/978-94-011-4930-3_30

Taylor, S.A., Larson, E.L., Harrison, R.G., 2015. Hybrid zones: windows on climate change. Trends Ecol. Evol. 30, 398–406. https://doi.org/10.1016/j.tree.2015.04.010

Toews, David P.L. Brelsford, A., 2012. The biogeography of mitochondrial and nuclear discordance in animals. Mol. Ecol. 21, 3907–3930. https://doi.org/10.1111/j.1365-294X.2012.05664.x

Tsaousis, A.D., Martin, D.P., Ladoukakis, E.D., Posada, D., Zouros, E., 2005. Widespread recombination in published animal mtDNA sequences. Mol. Biol. Evol. 22, 925–933. https://doi.org/10.1093/molbev/msi084

Ujvari, B., Dowton, M., Madsen, T., 2007. Mitochondrial DNA recombination in a free-ranging Australian lizard. Biol. Lett. 3, 189–192. https://doi.org/10.1098/rsbl.2006.0587

Van Oppen, M.J.H., McDonald, B.J., Willis, B., Miller, D.J., 2001. The evolutionary history of the coral genus *Acropora* (Scleractinia, Cnidaria) based on a mitochondrial and a nuclear marker:

1030 reticulation, incomplete lineage sorting, or morphological convergence? Mol. Biol. Evol. 18, 1315–
1031 1329. https://doi.org/11420370
1032 Veron, J.E.., 1995. J. E. N. Veron, 1995. Corals in space and time: the biogeography and evolution of
1033 the Scleractinia. Cornell Univ. Press. https://doi.org/10.1017/S0016756800008050
1034 Veron, J.E.. E.N., 2002. New Species Described in Corals of the World. Science. 11, 205.
1035 Vollmer, S. V., Palumbi, S.R., 2002. Hybridization and the evolution of reef coral diversity. Science.
1036 296, 2023–2025. https://doi.org/10.1126/science.1069524
1037 White, D.J., Wolff, J.N., Pierson, M., Gemmell, N.J., 2008. Revealing the hidden complexities of
1038 mtDNA inheritance. Mol. Ecol. 17, 4925–42. https://doi.org/10.1111/j.1365-294X.2008.03982.x
1039 Willis, B.L., van Oppen, M.J.H., Miller, D.J., Vollmer, S. V., Ayre, D.J., 2006. The role of hybridization
1040 in the evolution of reef corals. Annu. Rev. Ecol. Evol. Syst. 37, 489–517.
1041 https://doi.org/10.1146/annurev.ecolsys.37.091305.110136
1042 Wilton, P.R., Zaidi, A., Makova, K., Nielsen, R., 2018. A population phylogenetic view of
1043 mitochondrial heteroplasmy. Genetics 208, 1261–1274.
1044 https://doi.org/10.1534/genetics.118.300711
1045 Wirth, C., Brandt, U., Hunte, C., Zickermann, V., 2016. Structure and function of mitochondrial
1046 complex I. Biochim. Biophys. Acta - Bioenerg. 1857, 902–914.
1047 https://doi.org/10.1016/j.bbabio.2016.02.013
1048 Wolff, J.N., Pichaud, N., Camus, M.F., Côté, G., Blier, P.U., Dowling, D.K., 2016. Evolutionary
1049 implications of mitochondrial genetic variation: mitochondrial genetic effects on OXPHOS
1050 respiration and mitochondrial quantity change with age and sex in fruit flies. J. Evol. Biol. 29, 736–
1051 747. https://doi.org/10.1111/jeb.12822

Figure 1.

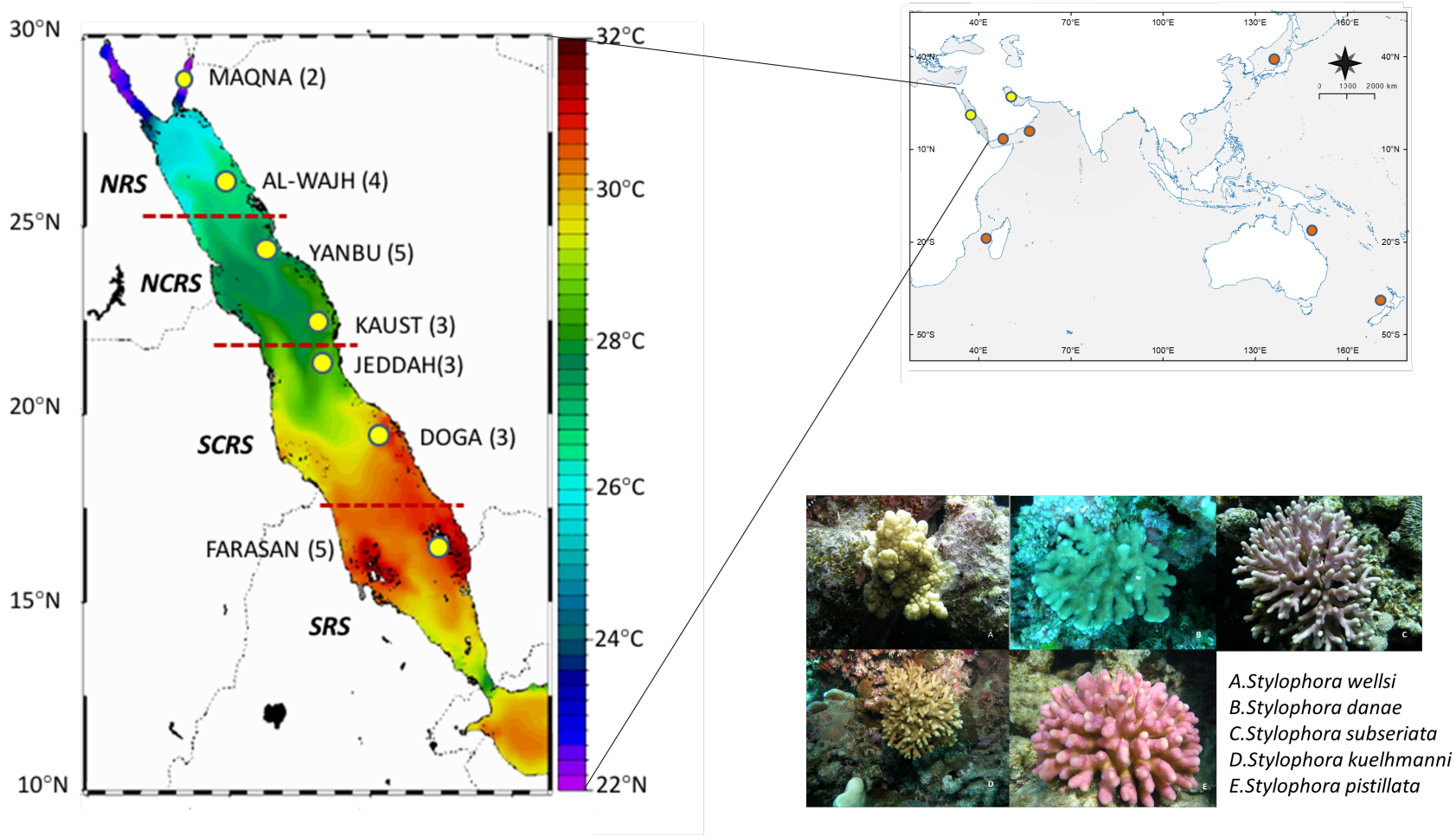

Sampling sites and *Stylophora* morphotypes collected in this study. Red Lines are indicating the barriers in oceanographic provinces described by Raitsos et al., (2013). Yellow points are sampling localities visited during this study. Reefs sampled in each location are included in parenthesis. Red points are sequences from other studies. The map was modified from the original downloaded from https://www7320.nrlssc.navy.mil/global_ncom/glb8_3b/html/Links/red/temp_glb8_3b_2012060700_0000m.gif

Figure 2.

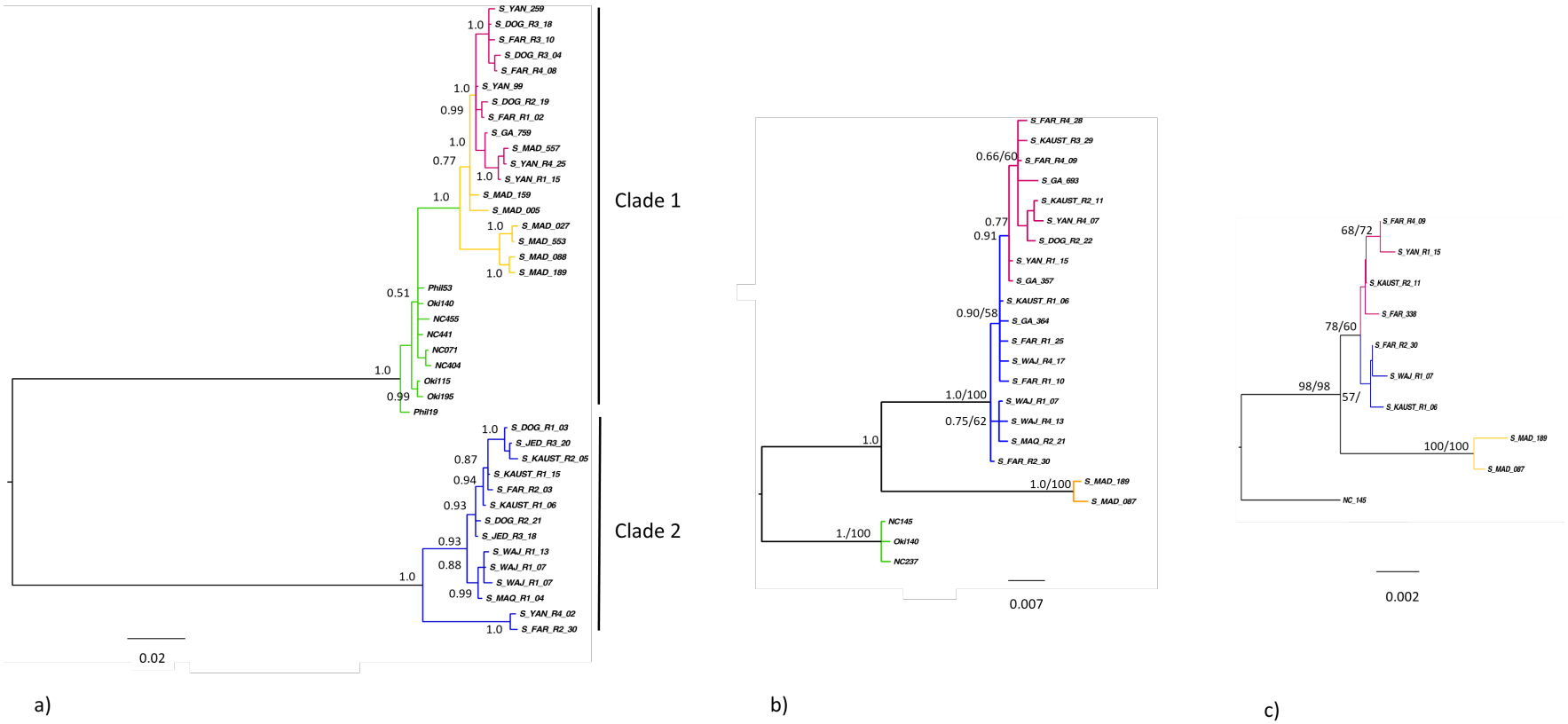

Mitochondrial phylogenies of the genus *Stylophora*. a). Bayesian tree of the *atp6*-mt*ORF* locus. b). Bayesian tree for the CR gene and c). Maximum Likelihood (ML) tree for the 12S gene. Node support are given in Bayesian Probabilities (BPP) for the mt*ORF*, BPP/ML for the mtCR and ML/NJ for the 12S. Colors are as follow: Red: Haplotypes from Arabian Gulf, Red Sea and Gulf of Aden placed in Clade 1 (*RS_LinA*). Yellow: haplotypes from Madagascar. Green: haplotypes from Indo-Pacific (Philippines, Okinawa, New Caledonia) and Blue: Red Sea and Gulf of Aden haplotypes placed in Clade 2 (*RS_LinB).* Haplotypes names are given in agreement to the region where the haplotype was found in higher frequency (MAQ=MAQNA, WAJ=ALWAJH, YAN=YANBU, KAUST = KAUST, JEDDAH=JED, DOG = DOGA, FARASAN = FAR).

Figure 3.

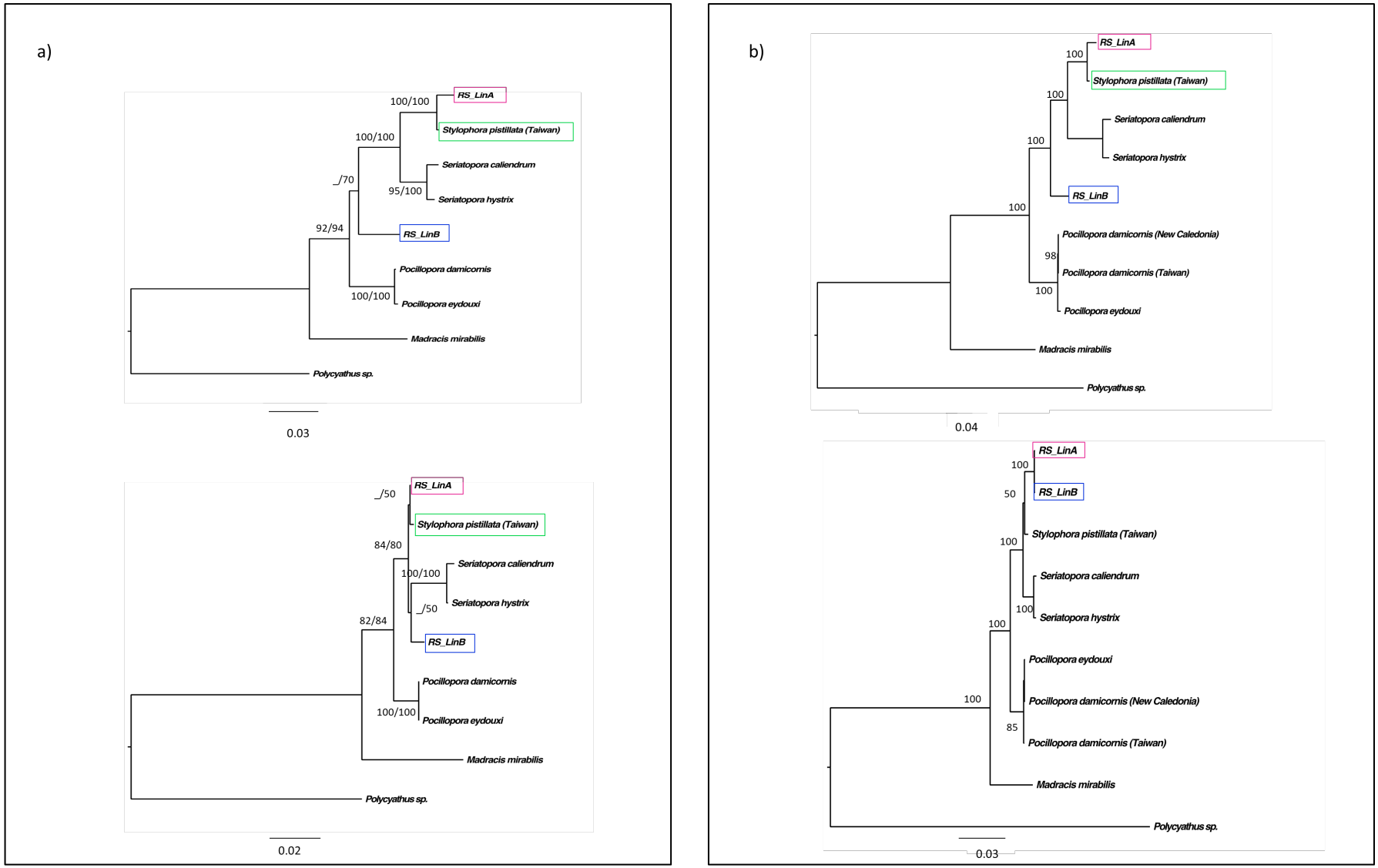

Mitochondrial phylogenies of the family Pocilloporidae and recombination analyses. a) Position of the *RS_LinA* and *RS_LinB* in a family phylogeny of the full *atp6* (above) and *nd6* genes (below). b). ML phylogenies from the recombination hypotheses: phylogeny derived from the recombinant region –minor parent–, including the *nd6*, *atp6*, and *mtORF* genes; 2415bp (above) and phylogeny from mtDNA genes outside the recombinant region –from the major parent – 9555bp (below).

Figure 4.

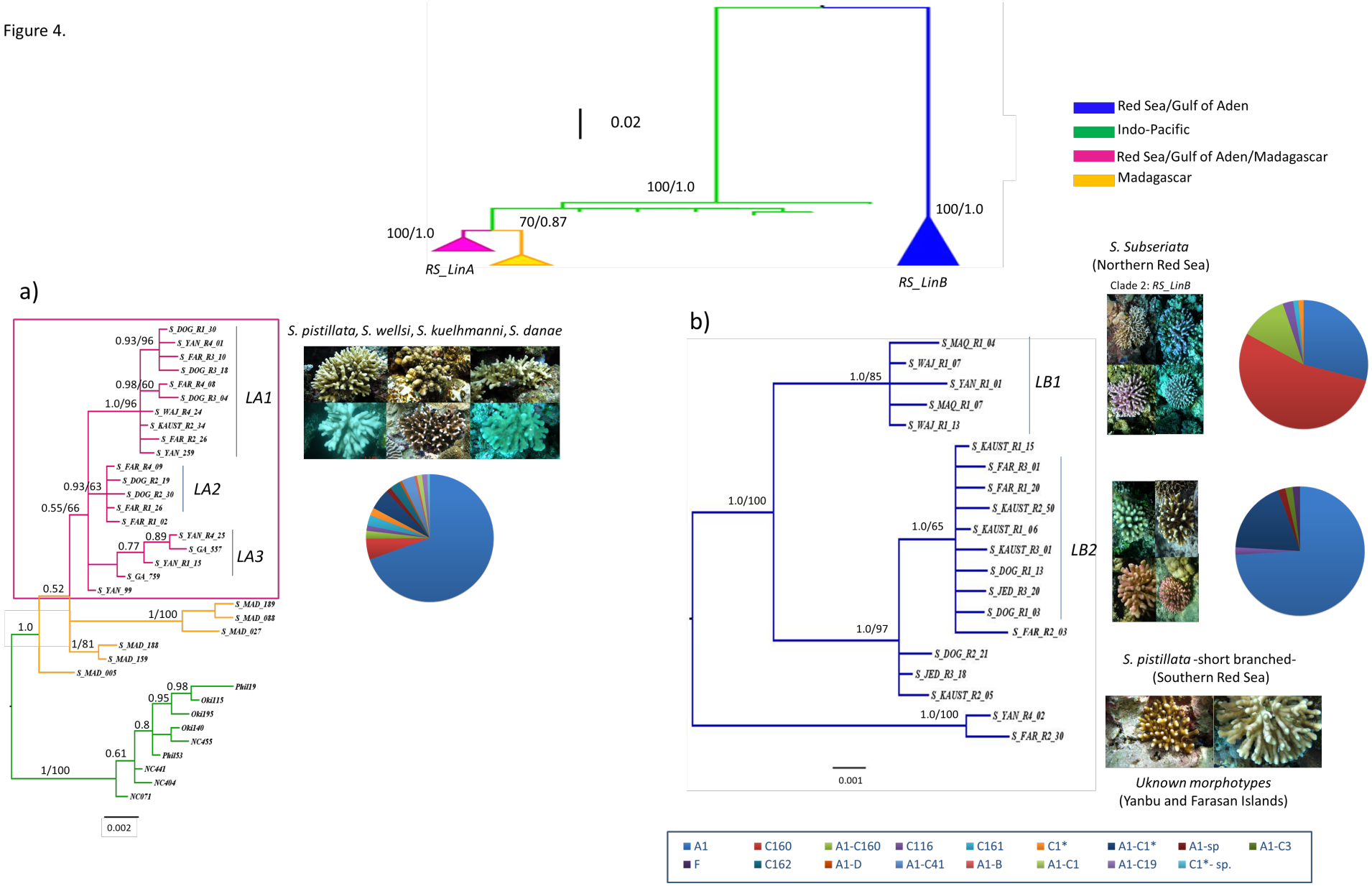

Extended *atp6*-mt*ORF* phylogenies for a). *RS_LinA* and b). *RS_LinB.* Morphotypes and *Symbiodinium* types associated with each lineage are shown.

Figure 5.

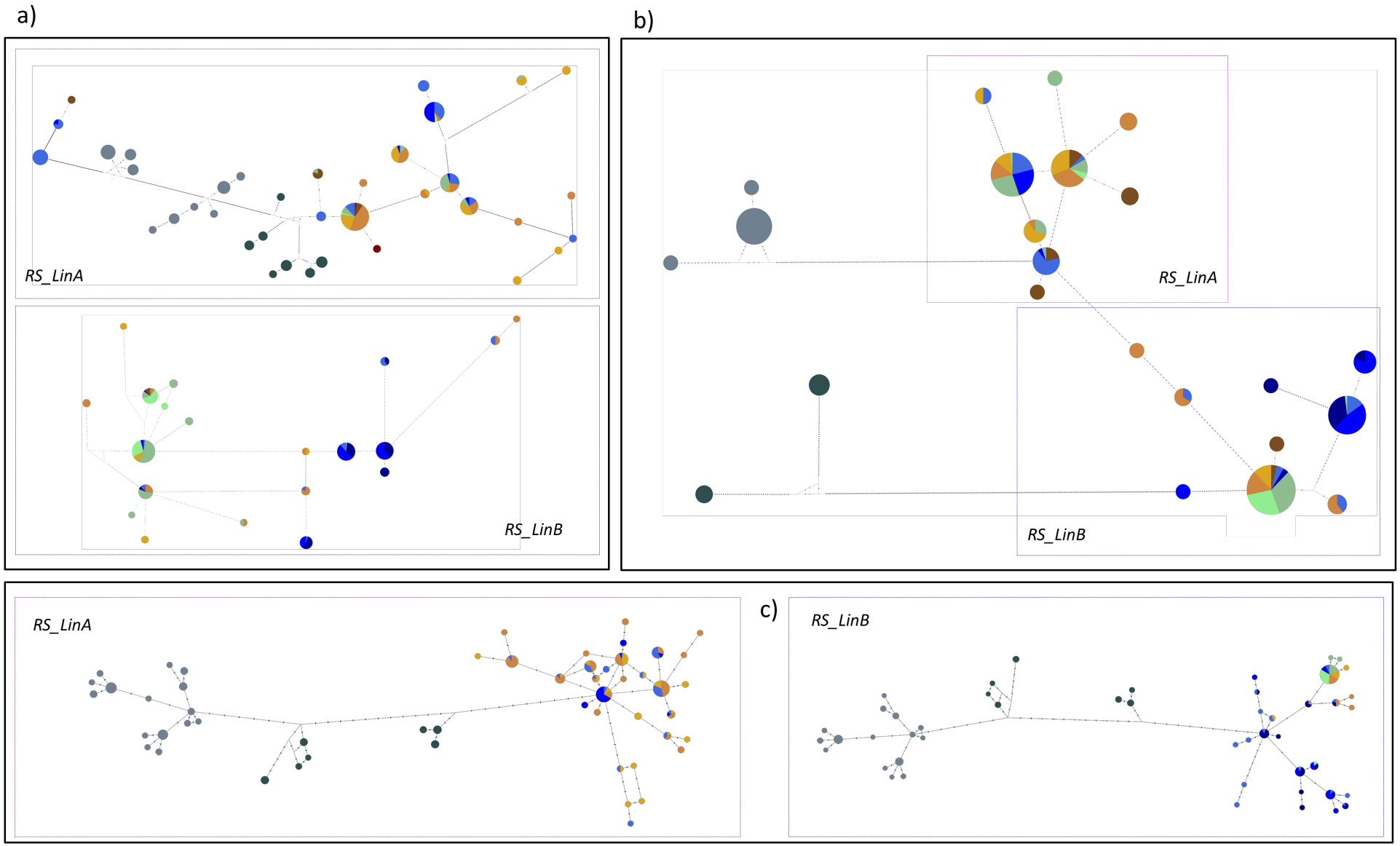

Network trees. a). *atp6*-mt*ORF* b). Control Region (CR) c). *hsp70.* Mutations are indicated as vertical lines.

Northern Red Sea
Central Red Sea
Southern Red Sea + Gulf of Aden
Madagascar
Pacific

Supplementary Figure *S1.*

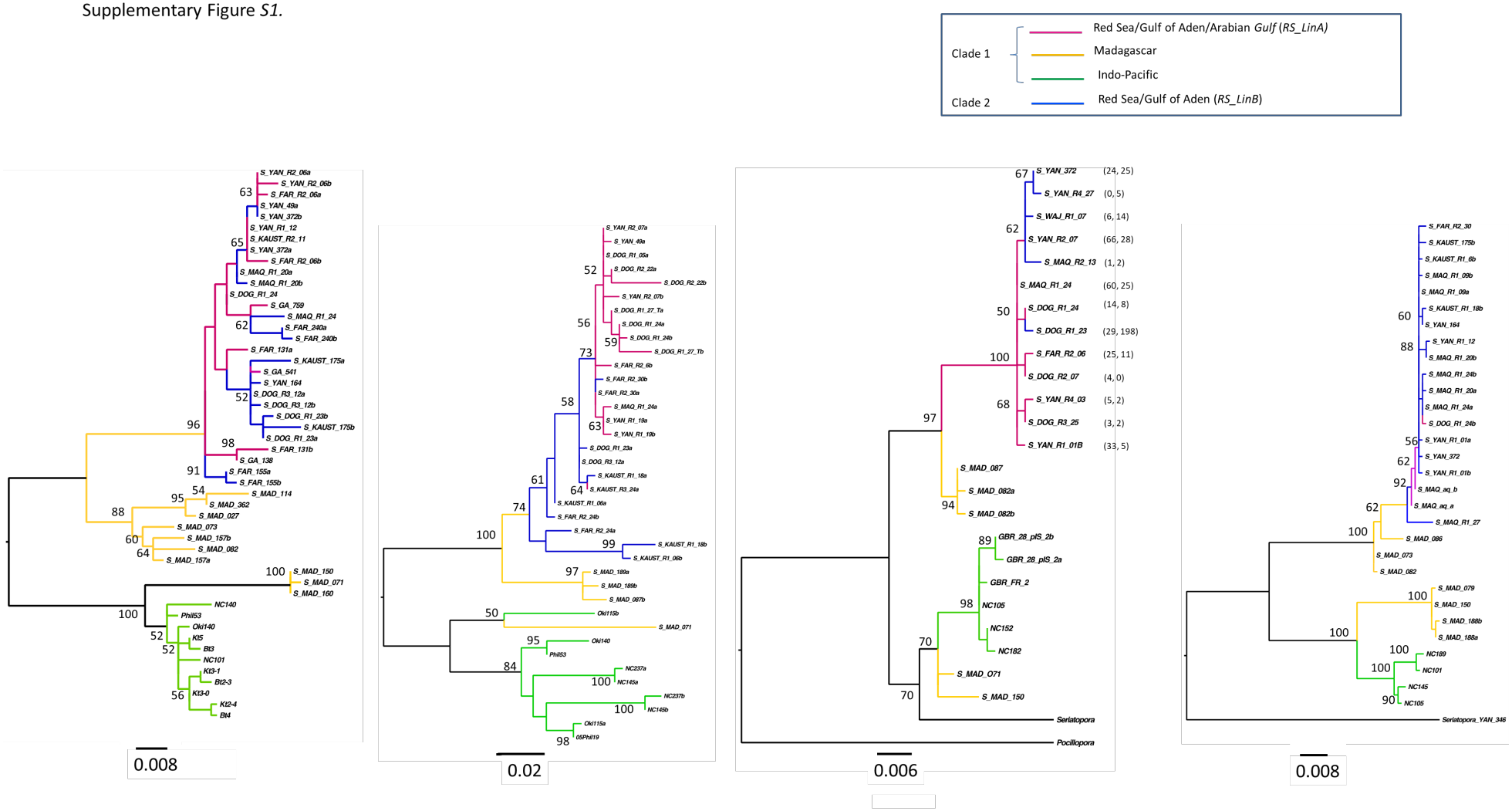

Nuclear phylogenies of the genus *Stylophora*. a). ITS1 b). ITS2 c). *hsp70* d). *PMCA*. Colors and haplotypes names are in agreement with those in the *atp6*-mt*ORF* phylogenies (see legend in Figure 2). In the *hsp70* phylogeny, the number of specimens found per haplotype in each lineage are placed within parentheses (*RS_LinA*, *RS_linB).*

Supplementary Figure *S2a*.

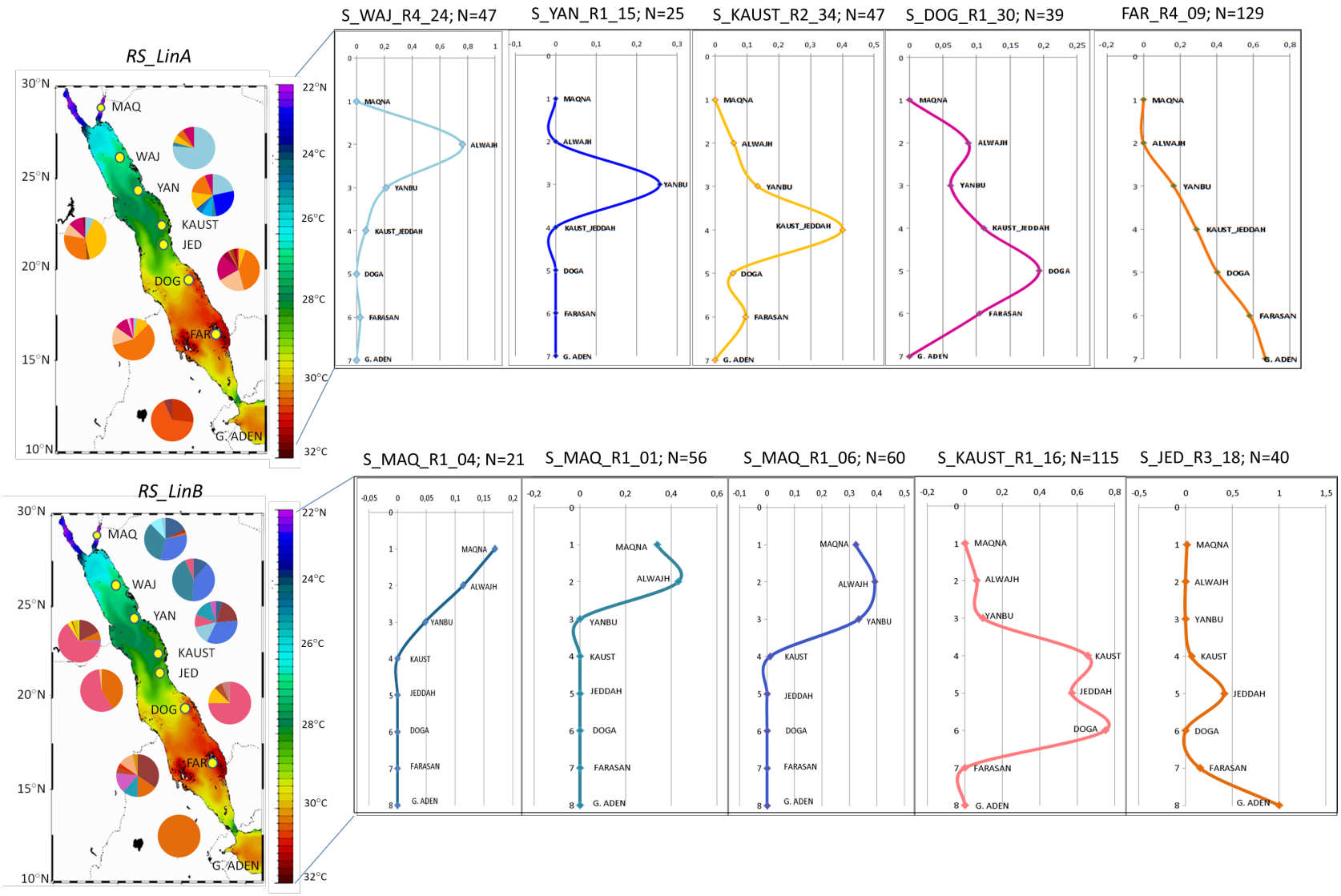

Distribution of haplotype frequencies along the gradient as per mtDNA lineage (*atp6*-mt*ORF* locus). Frequencies are indicated for the most common haplotypes. Axis x=relative frequencies.

Supplementary Figure *S2b*.

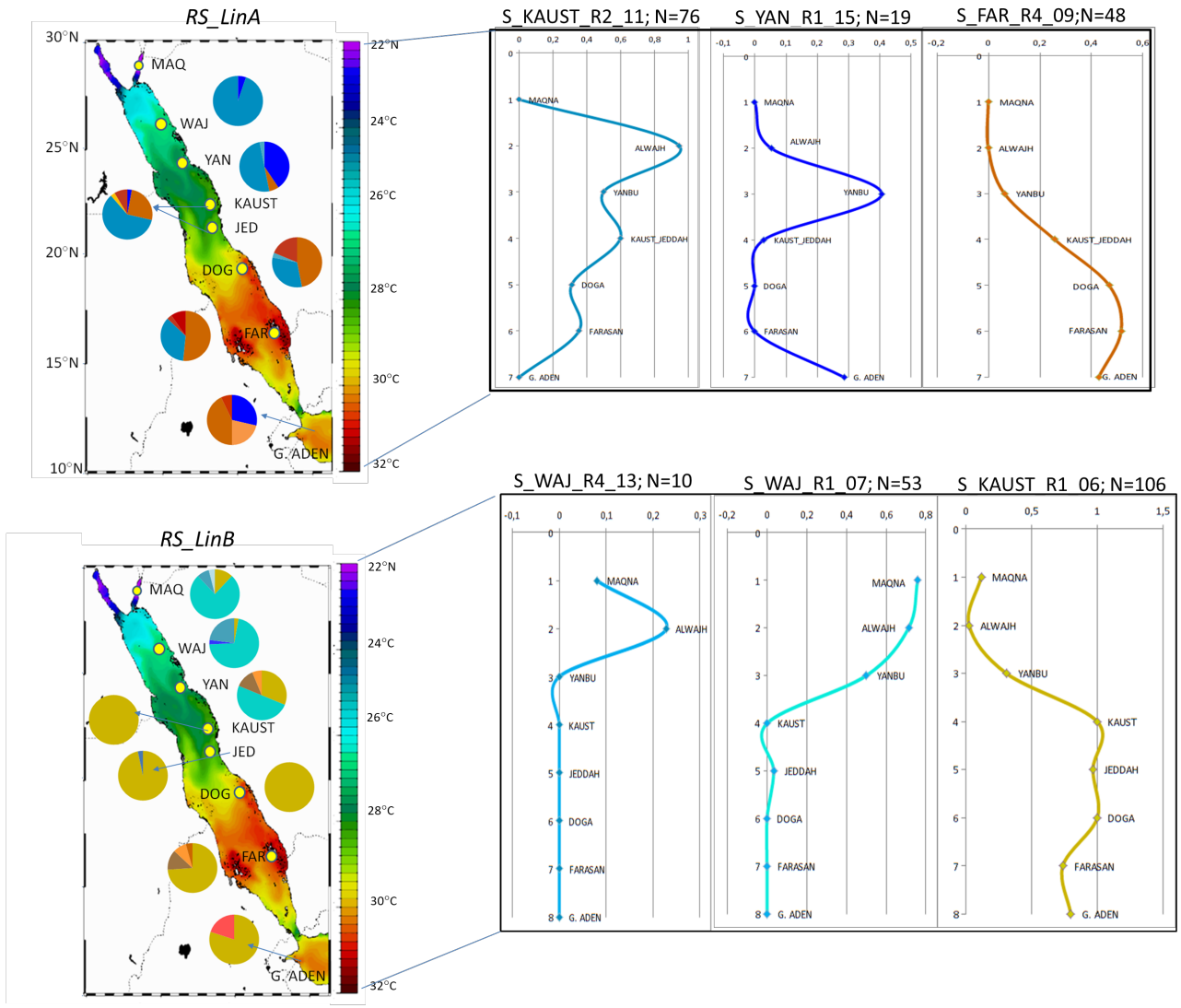

Distribution of haplotype frequencies along the gradient as per mtDNA lineage (CR fragment). Frequencies are indicated for the most common haplotypes. Axis x=relative frequencies.

Supplementary Figure *S2c.*

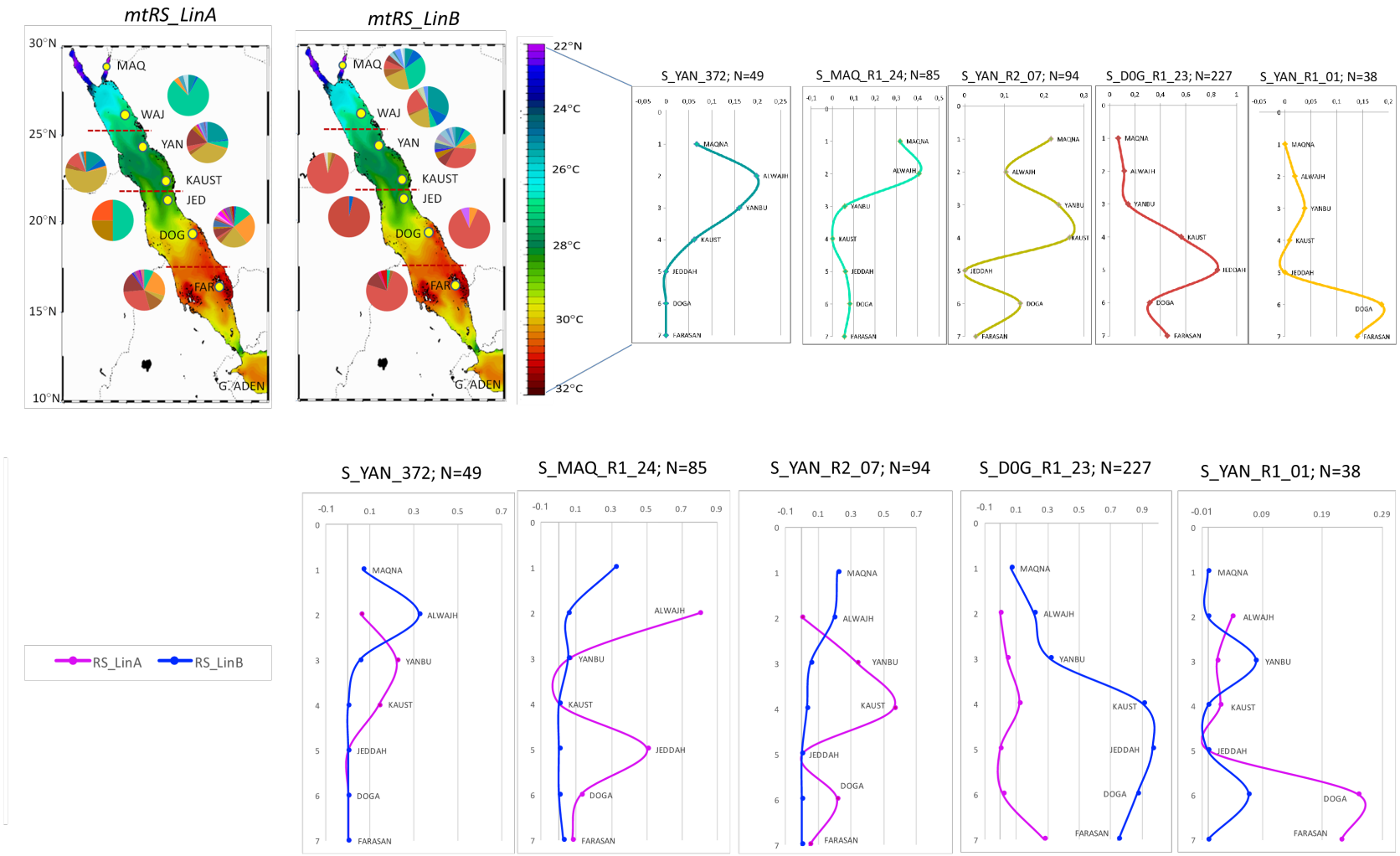

Distribution of haplotype frequencies along the gradient (*hsp70* fragment). Haplotype frequencies of the most common haplotypes (above) and in agreement with mtDNA lineages (below). Axis x=relative frequencies.

Supplementary Figure *S3*.

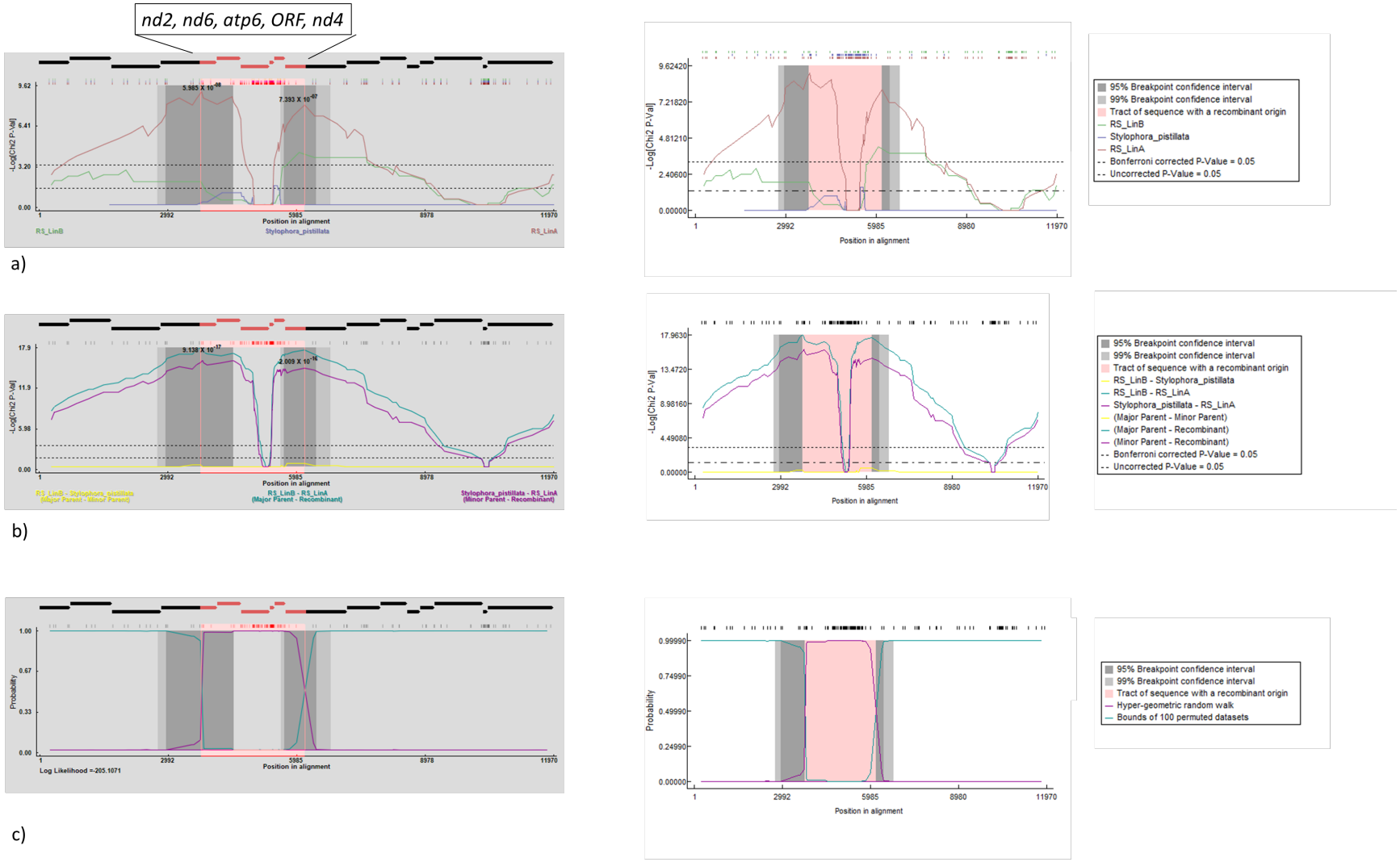

Recombination analyses. Identification of recombinant sequences and estimation of break points by different recombination methods. a). CHIMAERA b). MAXCHI and c) BURT.